

### الجمهورية الجزائرية الديمقراطية الشعبية People's Democratic Republic of Algeria وزارة التعليم العالي و البحث العلمي Ministry of Higher Education and Scientific Research المدرسة الوطنبة العليا للتكنولوجيات المتقدمة National Higher School of Advanced Technologies



Department of Electrical Engineering and Industrial Computer Science

# Final year project to obtain the diploma of Engineering

# Filed **Telecommunications**

 ${\bf Speciality}$   ${\bf Telecommunication~systems~and~networking}$ 

### Subject

# Design and implementation of an L-band voltage controlled oscillator

### Realized by AKHZEROUN Aimen

### Examination committee

DERMOUCHE Reda	Chair	ENSTA	MCA
BOUCHACHI Islem	Supervisor	ENSTA	MCA
ATROUZ Brahim	Examiner	ENSTA	MAA
BEGHAMI Sami	Examiner	ENSTA	MAA

Academic year: 2024-2025

### Dedication

As it cometh to be a kind of recognition, this thesis is dedicated to my parents, to my brothers, to my friends, to people who supported me out of their pure emotion, to people who helped me even with their words within my study course, I say your effort did not go in vain, may Allah bless you all and guide you through the rest of your life.

Acknowledgm	
As it cometh to be out of respect and high manners, I acknowle the material we needed to perform the realization of both of the by my supervisor, Mr.BOUCHACHI Islem, I admit his series	e projects, I also acknowledge every effort spent
	My hand will perish and its works will remain
	Ali Ben Mohamed AKHZEROUN

### ملخص

يتناول هذا البحث تصميم وتطوير جهاز ميكروويفي يتمثل في مذبذب يتم التحكم فيه عن طريق الجهد (VCO) مخصص لتطبيقات نطاق التردد L. يتضمن العمل أربعة فصول تغطي تقنيات مذبذبات الميكروويف المختلفة، ومبدأ عملها، ونتائج المحاكاة، بالإضافة إلى تحقيق النموذج العملي باستخدام خطوط نقل ميكروستريب ومكونات إلكترونية مُثبتة سطحيًا (SMD). كما تمت مناقشة مقارنة شاملة بين النتائج النظرية (المحاكاة) والنتائج التجريبية (القياسات). يعمل المذبذب المقترح ضمن نطاق ترددي يتراوح بين 1 جيجاهرتز و1.65 جيجاهرتز، وهو نطاق يتميز بضعف التأثر بالتوهين الجوي، مما يجعله مناسبًا لتطبيقات الرادار بعيدة المدي.

الكلمات المفتاحية: مذبذب يتم التحكم فيه عن طريق الجهد (VCO)، النطاق الترددي L رادار،الميكروستريبات ، مكونات إلكترونية، الجهاز الميكروويغي.

### Abstract

This thesis has known the proposition of a microwave device that is a voltage controlled oscillator for L-band applications, the document included four chapters in which we have discussed various microwave VCO technologies, their principle of operation, simulation and its results, and finally the realization of the device using microstrip transmission lines and Surface Mounted Device SMD components, a discussion took place to compare simulation to measurement results. The proposed VCO operates from 1GHz up to 1.65GHz, that is a band with high immunity to atmospheric attenuation which makes it suitable for Long range radar systems.

**Keywords:** Voltage-Controlled Oscillator (VCO), L-Band, Radar, Microstrips, Electronic components, Microswave device.

### Résumé

Ce travail de recherche porte sur la conception et le développement d'un dispositif micro-onde, à savoir un oscillateur commandé en tension (VCO), destiné aux applications dans la bande L. Le mémoire est structuré en quatre chapitres couvrant les différentes technologies des VCO micro-ondes, leur principe de fonctionnement, les résultats de simulation, ainsi que la réalisation pratique du dispositif en utilisant des lignes de transmission microstrip et des composants montés en surface (SMD). Une comparaison détaillée entre les résultats de simulation et les mesures expérimentales a également été effectuée. L'oscillateur proposé fonctionne dans une plage de fréquences allant de 1 GHz à 1,65 GHz, une bande réputée pour sa forte immunité à l'atténuation atmosphérique, ce qui la rend particulièrement adaptée aux systèmes radar longue portée.

Mots-clés: Oscillateur contrôlé en tension (VCO), Bande L, Radar, Microstrips, Composants électroniques, Dispositif micro-ondes.

## Contents

Li	st of	figure	es es	j
Li	st of	tables	3	iii
Li	st of	acron	yms	iv
In	trod	uction		1
1	Intr	roduct	ion and state of the art	2
	1.1	Introd	luction to Voltage Controlled Oscillators	. 2
	1.2	Histor	rical background and evolution of VCOs	. 3
	1.3	Impor	rtance of VCOs in microwave applications	. 3
		1.3.1	Electronic jamming equipment	. 3
		1.3.2	Function and waveform generator	. 3
		1.3.3	Phase locked loop	. 4
		1.3.4	Importance of voltage controlled oscillators	. 4
	1.4	Overv	riew of existing VCO technologies	. 4
		1.4.1	Stripline technology	. 5
		1.4.2	Microstrip technology	. 5
		1.4.3	CMOS technology	. 7
		1.4.4	Waveguide technology	. 8
	1.5	Recen	at advancements in VCO design	. 9
<b>2</b>	Pri	nciples	s of Operation and VCO Types	11
	2.1	Basic	working principle of a VCO	. 11
		2.1.1	Linear feedback model	. 11
		2.1.2	Negative resistance model	. 12
	2.2	Key p	performance parameters	. 13
		2.2.1	Phase noise	. 13
		2.2.2	Tuning range	. 17
		2.2.3	Frequency pushing and pulling	. 17
		2.2.4	Harmonic output power	. 18
		2.2.5	Power consumption	. 18
	2.3	Classi	fication of VCOs	. 18
		2.3.1	LC-tank VCOs	. 18
		2.3.2	Ring oscillator VCOs	. 20
		2.3.3	Colpitts and Hartley VCOs	. 22
		2.3.4	Dielectric Resonator Oscillators DROs	. 23
		2.3.5	MEMS-based VCOs	. 25
		2.3.6	Quartz oscillators	. 26

**28** 

 $3\,\,$  Design and Simulation of the Proposed VCO

3.1	Specification and design requirements	28
3.2	Simulation tools and methodologies: ADS	29
3.3	Selection of topology and components	30
	3.3.1 Amplifier design	30
	3.3.2 Resonator design	31
3.4	Circuit design and modeling	33
	3.4.1 Stability of the amplifier:	33
	3.4.2 Circuit design	33
3.5	· · · · · · · · · · · · · · · · · · ·	36
	3.5.1 Oscillation conditions verification	36
	3.5.2 Steady-state detection	36
	3.5.3 VCO transfer function	36
	3.5.4 Output power	37
	3.5.5 Phase and amplitude noise	38
	3.5.6 Figure of merit	38
3.6		39
	3.6.1 LPF circuits and responses	
4 Im	plementation, results, and discussion	42
4.1	Fabrication process	42
	4.1.1 Layout printing and component soldering	42
4.2		
	4.2.1 LPF measurements	43
	4.2.2 VCO measurements	44
4.3		48
Conclu	usion	49

# List of Figures

1.1	Linear feedback system	2
1.2	A basic block diagram of a phase locked loop	4
1.3	Cross section of a stripline transmission line	E
1.4	Field distribution in a stripline transmission line	5
1.5	Stripline voltage controlled oscillator	6
1.6	Cross section of a microstrip transmission line	6
1.7	Field distrubution a microstrip transmission line	6
1.8	Microstrip voltage controlled oscillator	7
1.9	CMOS voltage controlled oscillator	7
1.10	Cross section of a hollow rectangular waveguide	8
1.11	Waveguide voltage controlled oscillator	8
2.1	Linear feedback system	11
2.1	Negative resistance system	
2.2	Ideal and real frequency spectrums	13
2.4 2.5	Typical oscillator phase noise curve	14
	Typical oscillator phase noise curve	16
2.6 2.7	Transfer function of a voltage controlled oscillator	16 17
	· · · · · · · · · · · · · · · · · · ·	
2.8	Pictorial describes oscillation types generated by means of an LC-tank VCO	19
2.9	Basic LC tank oscillator	19
2.10	( ) 1	20
	A typical ring oscillators	20
	Pictorial represents the time to phase delay conversion	21
	Hartley and colpits oscillators	22
	Dielectric resonator oscillator	23
	Dielectric resonator equivalent circuit	24
	S <sub>21</sub> parameter of a dielectric resonator	25
2.17	Equivalent MEMS oscillator	25
3.1	EMpro environment	29
3.2	FEM simulator	29
3.3	Proposed push push amplifier	30
3.4	Simulated gain modes variations with respect to frequency	31
3.5	Resonator circuit	31
3.6	Frequency response of the resonator using lumped capacitors	32
3.7	Varactor diodes resonator	32
3.8	Frequency response of the resonator using varactor diodes	32
3.9	· · · ·	
	Push push amplifier stability	33
3.10	Push push amplifier stability	$\frac{33}{35}$

3.12	Steady state signals detected during simulation	36
3.13	Transfer function of the VCO	37
3.14	Output power of the VCO	37
3.15	VCO noise	38
3.16	Figure of merit of the VCO	38
3.17	Filter schematics	39
3.18	Filter responses	39
3.19	Layout design of the butterfly LPF	40
3.20	Momentum EM response of the butterfly LPF	40
3.21	Layout design of the VCO	41
4.1	Photolithography masks	42
4.2	Board material	42
4.3	Photolithography printing steps	43
4.4	Printed circuits	43
4.5	LPF measurement setup	44
4.6	NanoVNA LPF measurement results: $S_{11}$ and $S_{21}$ parameters	44
4.7	VCO measurement setup	44
4.8	Spectrum analyser VCO measurement results: Output frequency and output power	45
4.9	Spectrum analyser VCO measurement results: Phase noise	46
4.10	Spectrum analyser VCO measurement results: transfer function and output power	47

# List of Tables

1.1	Comparative analysis of key performance parameters of different VCO types including: Ring, LC, Class-B, Class-C,	
	Class-D, Class-E, and Colpitt's VCOs.	ć
3.1	Specifications of the proposed VCO	28
4.1	Material characteristics	43
4.2	Simulated and measured phase noise comparison	47
4.3	Comparative table between real world and the proposed device	48

### List of acronyms

ADS Advanced Design System

**BJT** Bipolar Junction Transistor

CMOS Complimentary Metal Oxide Semiconductor

CMRR Common Mode Rejection Ratio

 $\mathbf{DR}$  Dielectric Resonator

**DRO** Dielectric Resonator Oscillator

**DUT** Device Under Test

EM Electro Magnetic

**ENBW** Equivalent Noise BandWidth

 ${f FET}$  Field Effect Transistor

FM Frequency Modulation

FMCW Frequency Modulated Continuos Wave

FOM Figure Of Merit

IC Integrated Circuit

ITU International Telecommunication Union

 $\mathbf{LPF}$  Low Pass Filter

MDS Microwave Design System

**MEMS** Micro Electro Mechanical System

MOSFET Metal Oxide Semiconductor Field Effect Transistor

**NPN** Negative Positive Negative

NMOS Negative-channel Metal Oxide Semiconductor

PCB Printed Circuit Board

 ${\bf PD}\,$  Phase Detector

PLL Phase Locked Loop

PMOS Positive-channel Metal Oxide Semiconductor

QVCO Quadrature Voltage Controlled Oscillator

RADAR Radio Detection And Ranging

**RBW** Resolution Band Width

 ${\bf RF}\,$ Radio Frequency

**SMD** Surface Mounted Device

**TBM** Tactical Ballistic Missile

 ${\bf TE}\,$  Transverse Electric

 $\mathbf{TEM}$ Transverse Electro Magnetic

 ${f TM}$  Transverse Magnetic

 $\mathbf{VCO}\ \mathrm{Voltage}\ \mathrm{Controlled}\ \mathrm{Oscillator}$ 

 $\mathbf{VNA}$  Vector Network Analyser

**UAV** Unmanned Aerial Vehicle

**UHF** Ultra High Frequency

### Introduction

As threats from Unmanned Aerial Vehicles UAV's, long range fixed wing air-crafts, and long range missiles emerges, new early warning and detection systems are developed such as long range radar systems, the latter are used as a countermeasure for the threats mentioned before.

Long and medium range detection systems are used to fulfill several missions such as: long range detection, UAV detection, Tactical Ballistic Missile TBM warning, maritime surveillance [1], and also dedicated track and ballistic missile search [2], as military applications. In the civilian domain they are used for air traffic control, satellite communications, and satellite navigation systems [3] [4]. The frequency band that is suitable for such applications is the band from 1-2GHz, 15-30cm in terms of wavelength. This band is known according to the International Telecommunication Union ITU nomenclature as the Ultra High Frequency UHF band, however in radar nomenclature it is known as L-band [5]. This frequency band is known for its good signal penetration through earth's atmosphere, it faces less interference from heavy rain as the wavelength is relatively larger than the large water droplet dimension, therefore it is suitable to be used for the systems mentioned above. One of the basic building blocks of such systems is the signal generator, this device is responsible of generating an electrical signal in the adequate frequency band which is the L-band, therefore a device that exhibits electrical signals within the L-band is proposed through this very thesis.

Narrowing down the field of view to microwave oscillators yield the idea of creating a circuit that oscillates at the band of GHz with a frequency sweep around the centre frequency, that is a device known as voltage controlled oscillator VCO, such a device is an advanced oscillator, the main distinction between them is that an oscillator produces one oscillation frequency, however a VCO is capable of producing a continuum of oscillation frequencies as the frequency is susceptible to voltage variations in such a device.

Through this document the reader is going to experience the process of constructing a microwave device which is a voltage controlled oscillator, starting by defining a goal to achieve as a final result, the goal comprises a variety of constraints which are: centre frequency of oscillations, tuning percentage *i.e.*: frequency tuning range, phase noise level, power consumption, output power level, figure of merit also known as the FOM, these are the key performance parameters that our VCO must achieve the adequate level at each one of them. after defining the intended goal, choosing a manufacturing technology is the next step, due to the fact of ease of manufacturing and availability of microstrip line Printed Circuit Board PCBs, microstrips are chosen as a technology to fabricate all the circuits in this thesis.

Now the simulation phase starts by choosing an adequate simulation software; choosing a simulator for electronic circuits is almost easy, however since the manufactured circuits through this thesis are microwave circuits, a software that is capable of mixing conventional electronic schematic simulation and Radio Frequency RF & microwave simulation have to be chosen, that software is going to be Keysight Advanced Design System ADS, which is a professional simulation tool used in the industrial domain to simulate high performance microwave circuits, this software shows its reliability by using real data for electronic components that makes them non-ideal, which increases the resemblance to real life results.

After validating simulation results, the fabrication phase starts by printing the PBC board using photolithography technique, then soldering all electronic components on it. The final step is measurement, which consists of performing tests upon the fabricated circuit then comparing to simulation results, a validation step at last has to take place to confirm that the intended goal is reached.

### Chapter 1

### Introduction and state of the art

### 1.1 Introduction to Voltage Controlled Oscillators

A VCO, is an unstable electronic circuit that the output signals frequency is controlled by a bias voltage applied to a reverse biased varactor diodes, these diodes fill the role of capacitors in the resonator, along with an inductor they form an LC tank circuit used as a feedback circuit.

A VCO is composed of two main parts, the amplifier which is feed by a DC voltage and has a quantity of noise generated internally, the other part is known as the resonator and is responsible for selecting the oscillation frequency from the internal noise spectrum generated by the amplifier. In fact we can think about the VCO from two aspects in order to understand its operating principle. The first aspect is to assume that the resonator is a black box who generates dumped oscillations at a specific frequency, the electronic device responsible for dumping signals amplitude is identified physically as a resistor, the goal here is to compensate that resistance in a manner that yields steady state oscillations, The device that may do good for such a task is an amplifier with negative resistance equals the resistance of the resonators resistor so they annihilate each other, under that condition steady state oscillations occur out of nothing at the output of the VCO.

Another approach is the linear feedback VCO, that is to think of it as a closed loop that contains an amplifier with a voltage gain "A" and an output phase " $\phi$ ", and a feed-back block that has a voltage attenuation factor " $\beta$ " and an output phase " $\psi$ ", under Barkhausen conditions 1.1 steady state oscillations occur. Digging deeper beyond those conditions, lead us to the approach explained before which is the "negative resistance approach", that is to say that both approaches co-exist.

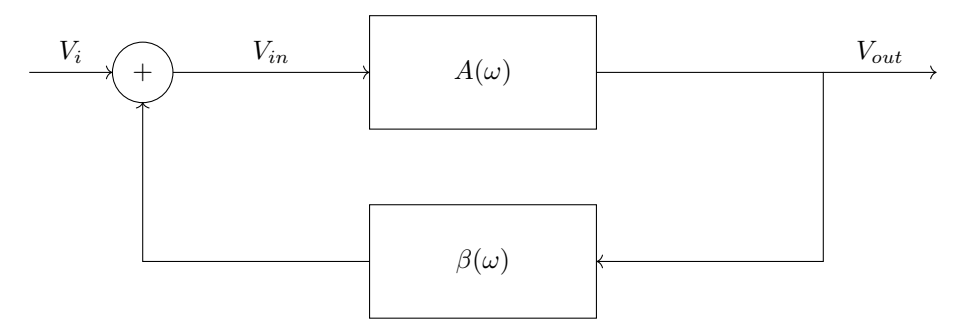


Figure 1.1: Linear feedback system

$$\begin{cases} A \cdot \beta = 1 \\ \psi + \phi = 0 \end{cases} \tag{1.1}$$

### 1.2 Historical background and evolution of VCOs

The scientific advancements during the late century in the filed of electromagnetism, laid the foundations for new technologies to rise such as: telecommunication systems, Radio Detection And Ranging RADAR systems, medical imaging devices based on electromagnetic waves radiation...ext, thus the need to develop electronic oscillators become primordial.

Before the year 1910, a device known as a spark gap oscillator was used to generate broadband signals [6], its working principle is to use a key such in Morse code transmission systems, once the key is closed a high voltage is applied to the spark gap in order to create a plasma flow across it, this plasma flow will ionize the air within the gap and the resistance will drop to  $2\Omega$  [7], a current is now drown continuously to the gap so it maintains arcing over. The constant plasma fluctuations occur rapidly, that means that the plasma current signal contains sever amplitude variations, consequently it has a broadband frequency spectrum. An antenna is used at the output as a selective device from this part, and from the other part as an electromagnetic radiator.

As the principle of super-heterodyne receivers was developed by Edwin H. Armstrong [8] in the year 1924, which is based on the heterodyne operation, that is to combine high frequency currents of two different frequencies to form a third frequency [9], based on this principle Armstrong used an early version of the vacuum tube known as Audion to manufacture an oscillator with steady state sinusoidal signal at the output. Improvements in vacuum tubes gave V.L Hartley the advantage to improve Armstrong's apparatus, where he increased its quality and expanded the range of frequencies [6], that is the beginning of voltage controlled oscillators.

By the invention of semiconductors in the late 1940's, electronic devices including voltage controlled oscillators has know a leap especially from the side of their size. By the invention of varactor diodes in 1961 by BARNES SANFORD H and MANN JOHN E, VCOs where taken to another level by improving their tuning capabilities [10].

The invention of new manufacturing techniques such as microstrips and striplines led to the development of new advanced voltage controlled oscillators with higher central frequencies, wider tuning ranges and lower phase noise, Nowadays VCOs are manufactured by means of Complementary Metal Oxide Semiconductor CMOS technology which is based on integration principle, as long as the size of semiconductors decreases new integration techniques are introduced, advanced VCOs are invented, which allows the researchers to achieve several hundreds of GHz and more [11].

### 1.3 Importance of VCOs in microwave applications

### 1.3.1 Electronic jamming equipment

Electronic jamming is a way of electronic warfare which represents the ability to use electromagnetic signals such as radio, infrared and radar signals, to disrupt, degrade and deny in some other systems to illude and deceive the adversaries ability to use their signals for their intended purposes [12]. The principle beyond jamming is to use artificially created interference offensively, that is to generate a signal at the same frequency band the opponent is using during transmission, or detection operations, the generated signal is then directed towards their antenna, the latter will absorb it and the system is jammed. Nevertheless frequency is important in jamming the amplitude play a crucial role too, as it is known that powerful signals omit weak once in terms of power by means of interference. The capability of frequency variation via voltage tuning possessed by voltage controlled oscillators makes its use primordial in such systems, that is because a jamming signal frequency must be tuned perfectly to match the enemy transmission frequency as the latter is an unknown information in these situations.

### 1.3.2 Function and waveform generator

A function or a waveform generator is an electric device which the purpose is to produce a variety of waveforms including sine waves, square and triangular waves over a wide frequency band. Its essential role is to be used

by engineers through design and testing procedures, to provide the input signal that is used to test electronic devices. A waveform generator must contain six main building blocks:

• Frequency controller.

• DC offset controller.

• Amplitude controller.

• Output connector.

• Waveform selector.

• Attenuator.

The component that may contain a voltage controlled oscillator is the frequency controller, that is used to adjust the frequency of the output signal which is the basic task accomplished by a VCO circuit [13].

### 1.3.3 Phase locked loop

A phase locked loop is a feedback system that compares the output to the input phase [14]. A basic PLL is composed of a Phase Detector PD, a VCO, and a Low Pass Filter LPF in a feedback loop topology as shown in figure:1.2.

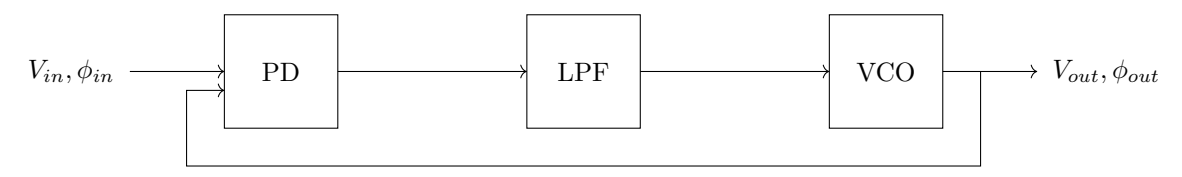


Figure 1.2: A basic block diagram of a phase locked loop

The phase detector will compare  $\phi_{in}$  to  $\phi_{out}$  and generate a signal called the phase error signal or the phase detector signal, the VCO will be driven by means of the PD signal in order to decrease the amount of phase error, that is phase locking. The low pass filter is used to filter high frequency components from the PD signal as the VCO is tuned by a steady state DC signal, consequently the usability of a voltage controlled oscillator lays in the fact of correcting phase error in a phase locked loop circuit.

### 1.3.4 Importance of voltage controlled oscillators

In summary voltage controlled oscillators are primordial circuits used in all telecommunication systems, the reason beyond this fact is, that telecommunication is a discipline based totally on periodic functions, these functions are used to carry data along the transmission channel as in data transfer for example in cellular networks or in satellite communication systems where we use a base band signal which is the useful information, and carry it on a sinusoidal signal known as the carrier, thus the need of a VCO in such systems is necessary as they are used to generate carrier frequencies. In other disciplines such as RADAR systems, where we do not need to modulate the carrier frequency basically, a pure sine is sent and the RADAR listens to the echo, this sine signal must be generated by means of a voltage controlled oscillator. As it is mentioned in section 1.3.3, VCOs are used in phase locked loops, a PLL is a circuit that locks the phase of a signal to achieve synchronization, it is used in FM receivers for example. It is now very clear that a voltage controlled oscillator is used all over electronic telecommunication circuits, from phones to automobiles, ground radars, embedded aircraft radars, along with other disciplines such as medical imagery that is based on electromagnetic waves radiation.

### 1.4 Overview of existing VCO technologies

Voltage controlled oscillators could be used in low frequencies and high frequencies, as this thesis is dealing with microwave band, the design of this VCO is necessarily done by means of microwave circuit technologies such as: striplines, microstrips, and CMOS technology, an overview of these technologies is going to have place in the next paragraphs.

### 1.4.1 Stripline technology

Stripline is a technology invented by Robert M.Barrett in the 1950s. Their structure is shown in figure:1.3, it consists of a conductor of thickness "t", width "W" in the center of a dielectric material of thickness "b", the dielectric is covered by ground planes from both sides of thickness "D".

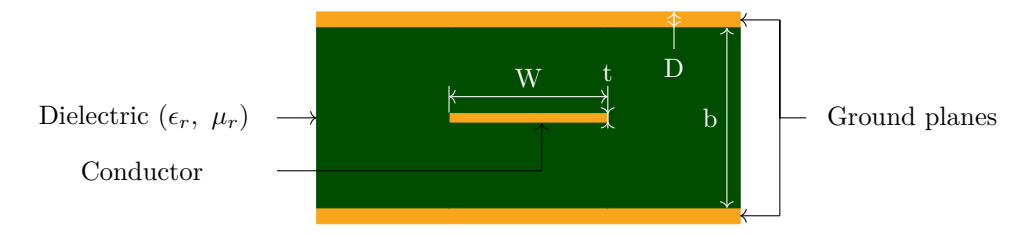


Figure 1.3: Cross section of a stripline transmission line.

The dominant mode of wave propagation in such lines is the transverse electromagnetic mode, its advantages are the non-dispersive behavior and frequency independent propagation, great isolation, and less radiation as the conductor is inside a dielectric medium.

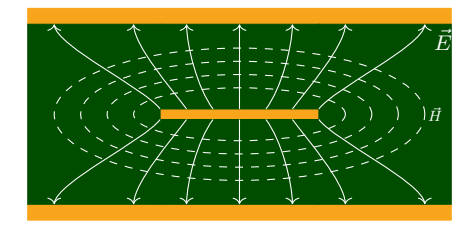


Figure 1.4: Field distribution in a stripline transmission line.

The characteristic impedance of striplines is given by the following approximation [15]:

$$Z_c = \frac{30\pi b}{\sqrt{\epsilon_r}(W_e + 0.441b)} [16] \tag{1.2}$$

According to [15] the effective width  $W_e$  is given by:

$$\frac{W_e}{b} = \frac{W}{B} - \begin{cases} 0 \text{ for } \frac{W}{B} > 0.35\\ (0.35 - \frac{W}{B})^2 \text{ for } \frac{W}{B} < 0.35 \end{cases}$$
 [16]

The design of transmission lines using stripline technology is complicated in comparison to microstrips, this is due to the sandwiched conductor inside the dielectric material, it is recommended as mentioned in [15] that the ground plane thickness is greater than five times the width of the conductor, this constraint have impact on the accuracy of characteristic impedance calculation and also it helps reducing the transverse radiation as shown in figure:1.4 from the document [16].

The exploitation of stripline in VCO design comes to the design of the transmission lines of the circuit using this technology, an example of such circuit is presented in figure:1.5 as a proof of case.

### 1.4.2 Microstrip technology

Microstrip transmission lines are widely used in microwave circuit design, their structure is way simpler than that of striplines which makes the circuit design easier using them, however this simplicity lead to a tradeoff between their efficiency and the design complexity. As shown in figuer:1.6, a microstrip transmission line is a conductor with width "W", thickness "t", laid on top of a dielectric material of thickness "h" as a mechanical

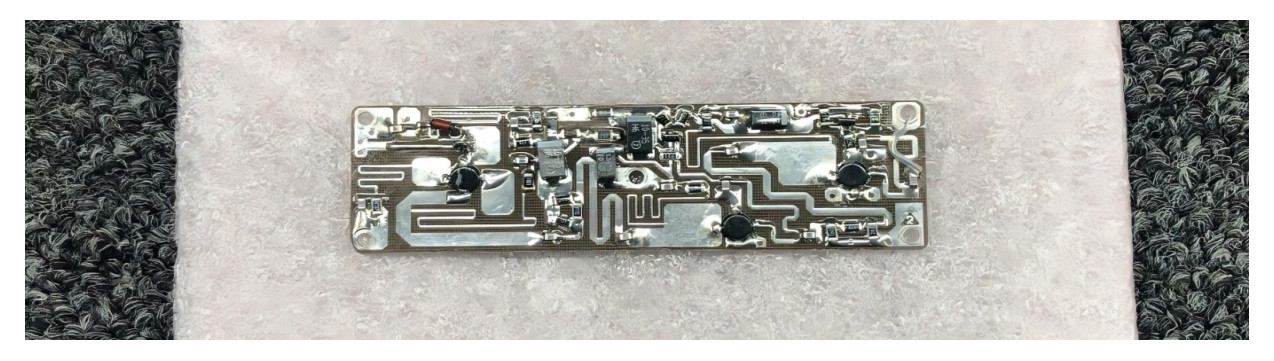


Figure 1.5: Stripline voltage controlled oscillator

parameter, and  $\epsilon_r$  and  $\mu_r$  as its electrical characteristics, under the dielectric material we have a ground plan, that serves as a reference to the waves traveling across the transmission line on top.

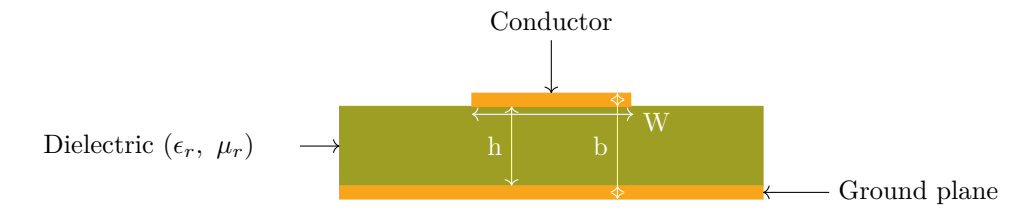


Figure 1.6: Cross section of a microstrip transmission line

The fact that the conductor which serves as the waves path, is in direct contact to air makes this transmission line structure susceptible to radiation, which leads to energy loss when we are dealing with circuits that are not based on radiation principle. Microstrip line support quasi-Transverse Electro Magnetic TEM propagation modes which is a hybrid mode of transverse electric and transverse magnetic modes [15], the reason beyond quasi-TEM is due to the fact that waves are partially guided through the dielectric material contrary to a waveguide or a stripline, which means that only a portion of the wave is guided through the dielectric, and that leads to the hybrid composition of Transverse Electric TE and Transverse Magnetic TM modes, also known as quasi-TEM mode.

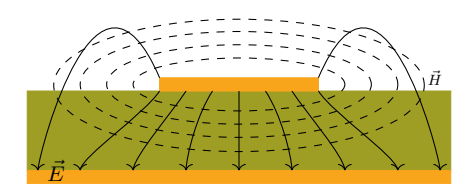


Figure 1.7: Field distrubution a microstrip transmission line

The effective dielectric constant  $\epsilon_{eff}$  and the characteristic impedance  $Z_c$  are given by the approximations stated in [15]:

$$\epsilon_{eff} = \begin{cases} \frac{\epsilon_r + 1}{2} + \frac{\epsilon_r - 1}{2} \left[ \sqrt{1 + 12 \frac{h}{W}} + 0.04 (1 - \frac{h}{W})^2 \right] \frac{W}{h} < 1 \\ \frac{\epsilon_r + 1}{2} + \frac{\epsilon_r - 1}{2} \sqrt{1 + 12 \frac{h}{W}} \frac{W}{h} > 1 \end{cases}$$
(1.4)

$$Z_{c} = \begin{cases} \frac{60}{\sqrt{\epsilon_{eff}}} ln\left(8\frac{h}{W} + 0.25\frac{W}{h}\right) \frac{W}{h} < 1\\ \frac{120\pi}{\sqrt{\epsilon_{eff}} \left[\frac{W}{h} + 1.393 + \frac{2}{3}ln\left(\frac{h}{W} + 1.444\right)\right]} \frac{W}{h} > 1 \end{cases}$$
 [16]



Figure 1.8: Microstrip voltage controlled oscillator

Figure:1.8 from [17], represents a piece of evidence on a voltage controlled oscillator manufactured using microstrip transmission lines technology.

### 1.4.3 CMOS technology

CMOS is the technology which consists of integrating field effect transistors inside an Integrated Circuit IC to serve several purposes, the transistors used in CMOS technology are Metal Oxide Semiconductor Field Effect Transistor MOSFET's of type Positive-channel Metal Oxide Semiconductor PMOS and Negative-channel Metal Oxide Semiconductor NMOS.

The complimentary aspect of CMOS circuits is based on the fact that it uses PMOS and NMOS transistors together in one design in an alternative operating mode, that is if PMOS is conducting the NMOS is blocking and vice versa. In comparison to conventional Bipolar Junction Transistor BJT circuits, CMOS counts many advantages such as: low power consumption, high integration density, and high noise immunity [18]. CMOS circuits are applied in several electronic domains, such as: digital logic circuits, system on chips, imaging sensors,...ext, but the one that is of interest to us is their application to microwave and RF circuits.

As technology is going faster towards compact designs like in mobile phones for example, where the whole motherboard surface is of several centimeters squared, the need to integrate RF electronic stages rises. The voltage controlled oscillator in figure:1.9 from [19], is a piece of evidence upon microwave CMOS circuits.

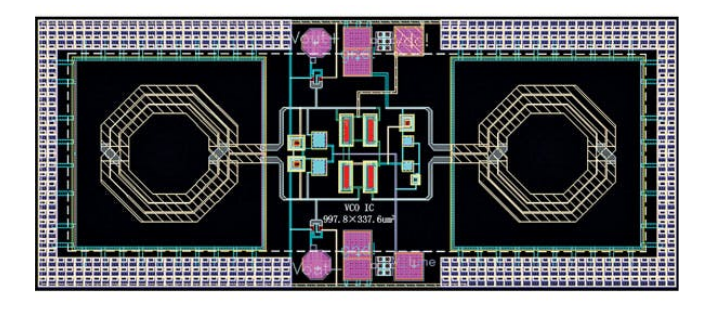


Figure 1.9: CMOS voltage controlled oscillator

### 1.4.4 Waveguide technology

A waveguide is either a hollow or dielectric filled metallic structure used to transport electromagnetic waves, waveguides come in many forms such as: circular and rectangular cross section waveguides, the most common one is the hollow rectangular waveguide as shown in 1.10, the circles represented at each corner are their for the sake of screw fixing, electromagnetic waves will travel inside the rectangle with dimensions "a" and "b", the propagation modes inside a waveguide are limited to TM and TE modes, both modes in this case have a lower cutoff frequency which is a function of the dimensions of the waveguide itself, and the electric characteristics of the inside dielectric [20], in the case of a hollow rectangular waveguide the dielectric is air, that is  $[\epsilon, \mu] = [\frac{1}{36\pi} 10^{-9} F \cdot m^{-1}, 4\pi \cdot 10^{-7} H \cdot m^{-1}]$ .

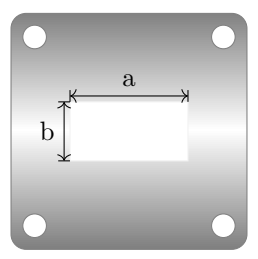


Figure 1.10: Cross section of a hollow rectangular waveguide

Propagation inside a waveguide is composed from multiple modes, the dominant mode and its high order modes, The lower cutoff frequency expression of transverse electric and transverse magnetic modes is given according to [20] by:

$$f_{c(m,n)} = \frac{1}{2\pi\sqrt{\epsilon\mu}}\sqrt{\left(\frac{m\pi}{a}\right)^2 + \left(\frac{n\pi}{b}\right)^2}$$
(1.6)

The lowest cutoff frequency of the combination (m, n) = (1, 0) for TE modes is:

$$f_{c(1,0)} = \frac{1}{2a\sqrt{\epsilon\mu}} [21]$$
 (1.7)

The lowest cutoff frequency of the combination (m, n) = (1, 1) for TM modes is:

$$f_{c(1,1)} = \frac{1}{2\pi\sqrt{\epsilon\mu}}\sqrt{\left(\frac{\pi}{a}\right)^2 + \left(\frac{\pi}{b}\right)^2} [21]$$
 (1.8)

Assuming that a > b and as the  $TE_{(1,0)}$  and  $TM_{(1,0)}$  are the modes with the lowest cutoff frequency, they are considered as the dominant propagation modes. figure:1.11 from [21] shows a waveguide VCO.

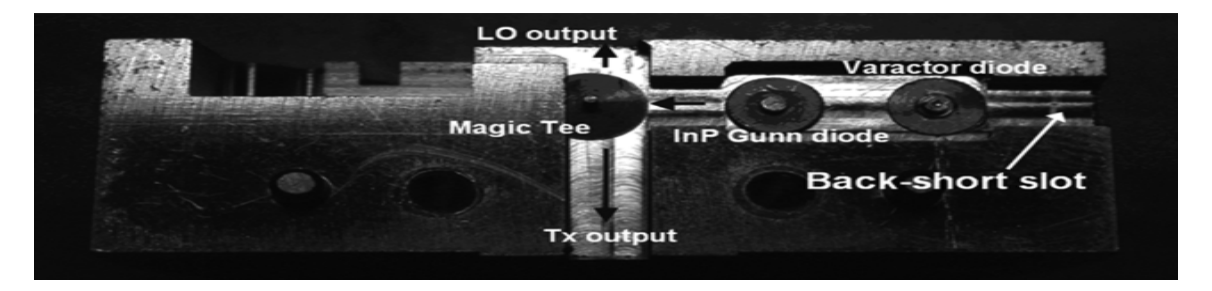


Figure 1.11: Waveguide voltage controlled oscillator

### 1.5 Recent advancements in VCO design

Advancements in electronic circuit manufacturing lead engineers to omit the use of large scale technologies such as microstrips and striplines, this is due to their inconvenience in energy dissipation as well as their huge size in comparison to other technologies such as CMOS technology. This very technology came to be exploited in RF and microwave circuits as its size in far way compact in comparison to conventional RF circuits, it consumes less power, and it produces less phase noise. Table:1.1 from [22] contains a comparative resume on key performance parameters of multiple VCO's.

Table 1.1: Comparative analysis of key performance parameters of different VCO types including: Ring, LC, Class-B, Class-C, Class-D, Class-E, and Colpitt's VCOs.

Year	Technol- ogy	VCO Type	Power supply (V)	Power consump- tion (mW)	Phase noise (dBc/Hz)	Offset frequency (MHz)	FOM (dBc/Hz)	Frequency (GHz)	Tuning range %
2022	90nm	Current	1.2	1.6	-90.26	1MHz	-155.8	2.4	96.26
		Starved							
2022	$180\mathrm{nm}$	Differ-	1.8	8.1	-86.7	$1 \mathrm{MHz}$	-149.7	5.4	34.00
		ential							
2022	$65\mathrm{nm}$	LC-	1.2	7.7	-115.35	$1 \mathrm{MHz}$	-183	7.4	29.9
		NMOS							
2019	28nm	LC-	0.9	9	-114.5	$1 \mathrm{MHz}$	-188	15.8	25
		PMOS							
2022	$65\mathrm{nm}$	LC-	1	11.1	-110.03	$1 \mathrm{MHz}$	-189.3	28.66	15.2
		CMOS							
2022	22nm	Class-B	1	14.4	-178.3	1MHz	-96.6	23.8	5
2022	130nm	Class-	1.4	3.08	-119.9	1MHz	-193.4	18.1	25.5
		B/Class-							
		$\mathbf{C}^{'}$							
2022	28nm	Class-D	0.56	0.054	-186.6	1MHz	-93.77	7.13	14.18
2022	180nm	Class-E	0.7	4.9	-187.6	100KHz	-115.3	4	10.6
2021	90nm	Col-	5	45	-192	$1 \mathrm{MHz}$	-137.44	3.4	4.5
		pitt's							

In the past two years VCO technology knew numerous advancements from several sides including size, compactness, phase noise, and power consumption, from these we can cite some works from the years 2021, 2022, and 2023 so the reader can have an idea about the recent advancements in this domain, from [22] it is stated in the taxonomy digrams:

- ring voltage controlled oscillators:
  - Chao et al,2023 developed an N stage ring VCO with improved phase noise, a reduced  $\frac{1}{f^3}$  corner concerning the Lessons phase noise diagram.
  - Kiloo et al,2023 developed a four stage differential VCO with a wide tuning range.
- NMOS LC voltage controlled oscillators:
  - Mohammed et al,2022 developed a wide tunable LC VCO with low supply voltage, low phase noise and steady output frequency.
  - Imran et al,2022 developed a Quadrature Voltage Controlled Oscillator QVCO that achieves very low phase noise levels, low power dissipation, and high Q factor.
- PMOS LC voltage controlled oscillators:
  - Mai et al, 2019 developed an LC PMOS VCO with low phase noise, and low power consumption.

- CMOS LC voltage controlled oscillators:
  - Sophia et al,2021 developed a cross coupled VCO that produces a better phase noise as well as a
    wide tuning range.
  - Hao Guo et al, 2021 used Muli-rosonant RLCM tank method to improve phase noise an the FOM.

Due to the fact that resent advancements if VCO technologies are manufactured by means of CMOS technology, a one might justify the use of BJT's later on in the proposed VCO design, this is due to the fact that CMOS manufacturing requires advanced machines which are currently not in our disposal, on the other hand the BJT transistors we intend to use are lumped components which means that dealing with them is easy in comparison with CMOS technology.

By mentioning these recent advancements chapter one is concluded, the next chapter will completely consecrated to principles of operation of various VCO technologies.

### Chapter 2

# Principles of Operation and VCO Types

### 2.1 Basic working principle of a VCO

The voltage controlled oscillator is a device that the working principle could be tackled from two points of view, or in other words modeling a VCO could be done using two approaches: the linear feedback approach, and the negative resistance approach. Both principles are to be explained through this chapter, thus the reader could build a strong idea about VCO's and understand how does they operate.

### 2.1.1 Linear feedback model

From the linear feedback model point of view, a voltage controlled oscillator is basically an unstable amplifier connected to a feedback loop, the working principle is that the amplifier once fed using a DC voltage, a white noise is generated internally due to the active components used to construct the amplifier circuit, the feedback network, is fed a portion of this noisy voltage, as it is known to be a selective passive circuit, the signal will be most likely filtered except the signal that the frequency meets the central frequency of the feedback network, more precisely only noise within the 3dB bandwidth of the transfer function of the selective feedback network is amplified [23], the filtered sine will be injected back into the amplifier, and the loop remains on that state under Barkhausen conditions of oscillation stated in 1.1. The output signal is now a pure sinusoidal signal.

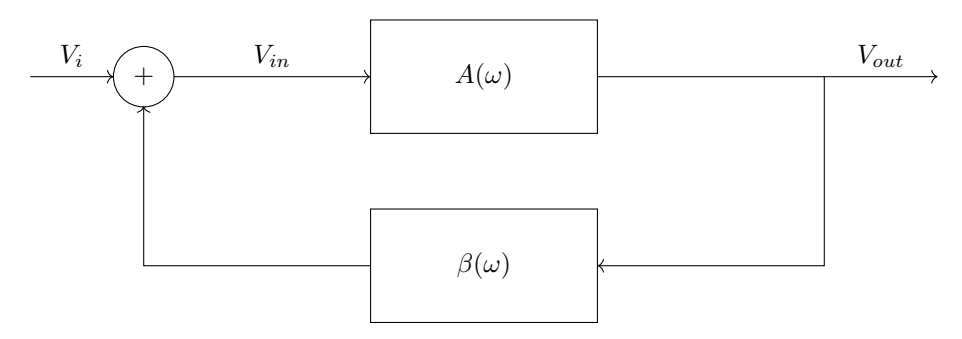


Figure 2.1: Linear feedback system

In figure:2.1, a linear feedback oscillator is represented, the amplifier is characterized by its voltage gain  $A(\omega)$  which is a function of the angular frequency  $\omega$ . The feedback network is characterized by its transfer function  $\beta(\omega)$ . It is now a good starting point to extract a relation between  $V_{out}$  and  $V_i$ : We have:

$$V_{in} = V_i + \beta(\omega)V_{out} \tag{2.1}$$

Then:

$$V_{out} = A(\omega)V_{in} \tag{2.2}$$

$$= A(\omega) [V_i + \beta(\omega)V_{out}]$$
 (2.3)

$$= \frac{A(\omega)}{1 - A(\omega)\beta(\omega)} V_i \tag{2.4}$$

Equation (2.4) depicts that at  $\omega = \omega_{OSC}$ , where the denominator becomes null, the output voltage tends to reach a practical high value, said theoretically as infinity, at this case it is possible for the output voltage to develop out of nothing, which means that the oscillation amplitude starts to develop from 0V until it reaches  $V_{OSC}$ , this is explained by the fact that oscillations are produced out of the broadband internal noise, which has a very low amplitude, as it is mentioned before, the noise outside the 3dB bandwidth of the feedback loop will be attenuated, and that explains the sinusoidal output of the oscillator at  $f = f_{OSC}$ . In fact the oscillator must firstly capture the initial phase as  $V_{out} = 0$  at an early time [23].

Observing equation 2.5 given by definition, it is very clear that the phase variation by time produces frequency at a  $\frac{1}{2\pi}$  considered constant.

$$f = \frac{1}{2\pi} \frac{d\theta}{dt} \tag{2.5}$$

Capturing the initial phase means possessing the starting point of oscillations as all periodic signals possess an initial phase that varies along time, however the oscillation frequency is fixed by means of the components used to construct the feedback loop, as their values tend to be small, the energy stored and exchanged between them will take a small exchange time, as frequency is by definition the inverse of time *i.e.* period, the frequency will tend to be very high, that explains the high frequency of microwave voltage controlled oscillators, it could be also explained as the very fast phase variations along time.

The oscillation condition for steady state oscillations is then derived easily from equation (2.4):

At  $\omega = \omega_{OSC}$  we have:

$$V_i \to \infty \Rightarrow 1 - A(\omega)\beta(\omega) = 0 \Rightarrow |A(\omega_{OSC})\beta(\omega_{OSC})| = 1$$
 (2.6)

for the phase the condition is:

$$Arg[\beta(\omega_{OSC})A(\omega_{OSC})] = Arg[1] \Rightarrow Arg[\beta(\omega_{OSC})] + Arg[A(\omega_{OSC})] = 0^{\circ}$$
(2.7)

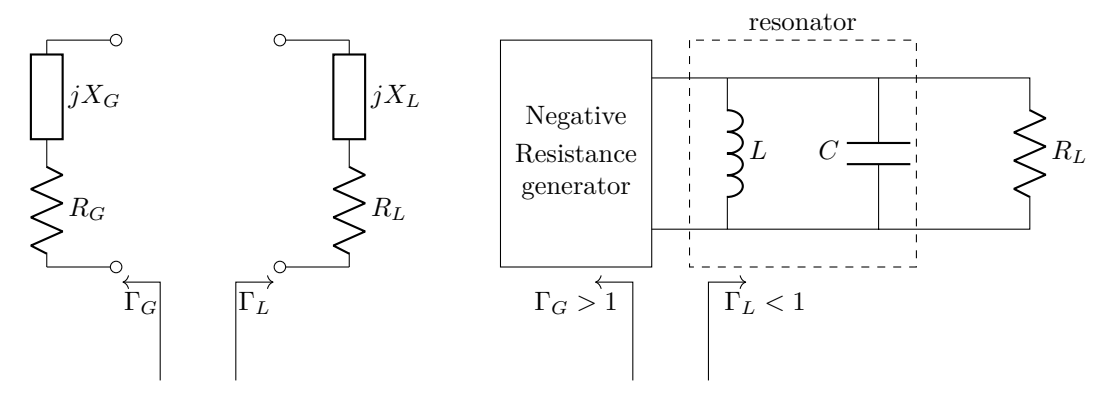
Then:

$$\begin{cases} |A(\omega_{OSC})\beta(\omega_{OSC})| = 1\\ Arg[\beta(\omega_{OSC})] + Arg[A(\omega_{OSC})] = 0^{\circ} \end{cases}$$
 (2.8)

### 2.1.2 Negative resistance model

From the negative resistance approach, a voltage controlled oscillator is a device that comprises two key components, the negative resistance generator, and the resonator tank load, this configuration works as the resonator will oscillate once fed as explained in the introduction, the issue here is that the oscillations are dumped because of the resistance of the resonator, this resistance is compensated by means of the negative resistance generator to produce steady state oscillations at the output.

The topologies represented in figure:2.2, are both of a negative resistance oscillator, from a point of view of reflection coefficients figure:2.2(b)  $\Gamma_L$  and  $\Gamma_G$ , the oscillation condition is that the magnitude of the reflection coefficient of the amplifier have to be greater than unity, and the reflection coefficient toward the resonator must



- (a) Oscillator model as Negative resistance
- (b) Negative feedback oscillator model

Figure 2.2: Negative resistance system

be less than unity, this is achieved automatically by preserving the following oscillation condition [24]:

$$\begin{cases} R_G + R_L = 0 \\ X_G + X_L = 0 \end{cases}$$
 [25]

### 2.2 Key performance parameters

### 2.2.1 Phase noise

It is by attitude to refer to an oscillator noise as phase noise, this is due to the fact that amplitude noise could be suppressed by the gain of the oscillator. Phase noise is a crucial performance parameter in a voltage controlled oscillator, because it is directly related to phase fluctuations of the output signal, phase fluctuations lead to frequency drifting as frequency is said to be the derivative of phase with respect to time at a given constant. Frequency drifting or in other words frequency variations that are caused by phase fluctuations may cause output signal distortions which leads to increase the bandwidth of its spectrum, that means to directly affect the purity of the output sinusoidal signal, that is as to say the output signal of the VCO is impure, while signals purity remains one of the primordial characteristics of a VCO, phase fluctuations must be suppressed in order to achieve pure sinusoidal signals.

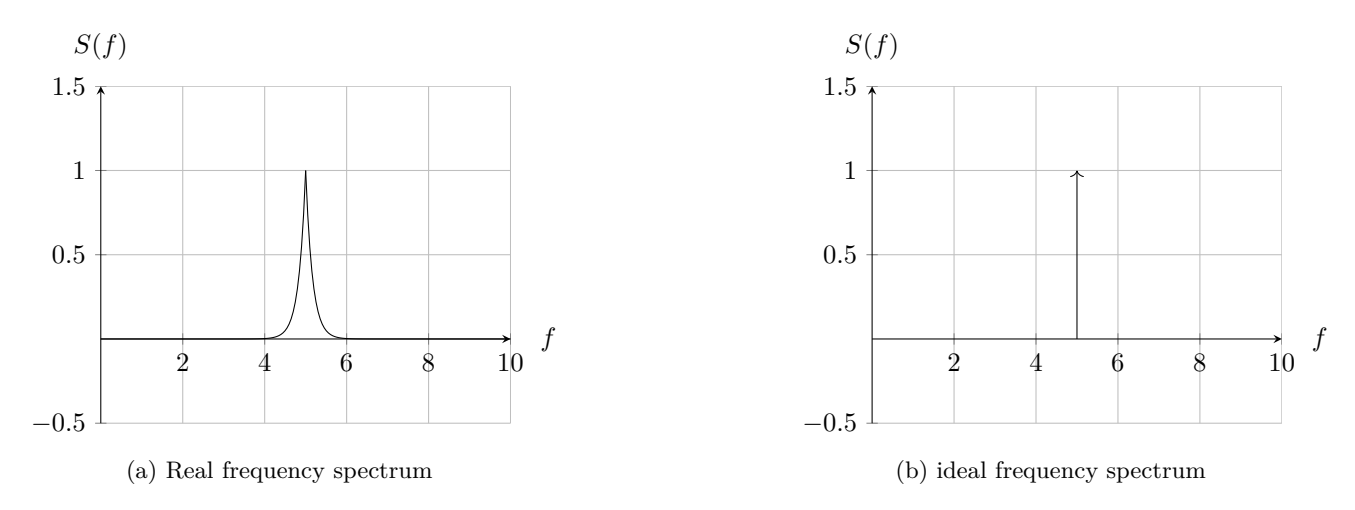


Figure 2.3: Ideal and real frequency spectrums

In figure: 2.3 we observe both ideal and real frequency spectrums, the ideal spectrum contain no sidebands that is to say no noise is affecting the time domain signal due to its ideality of course, however the real frequency spectrum contains sidebands that are due to several kinds of noise which are: phase noise, flicker noise, and

thermal noise. These sidebands are the cause of sinusoidal impurity in signal generation cases as in local oscillators or in transmitters, these sidebands contain energy that may affect nearby weak channels [25].

As phase noise is of great importance to VCO design, a figure of merit has been defined by Professor David B.Leeson in the year 1966 [26], this phase noise curve model serves as a reference to VCO designers, the figure of merit or the typical phase noise plot is shown in figure:2.4.

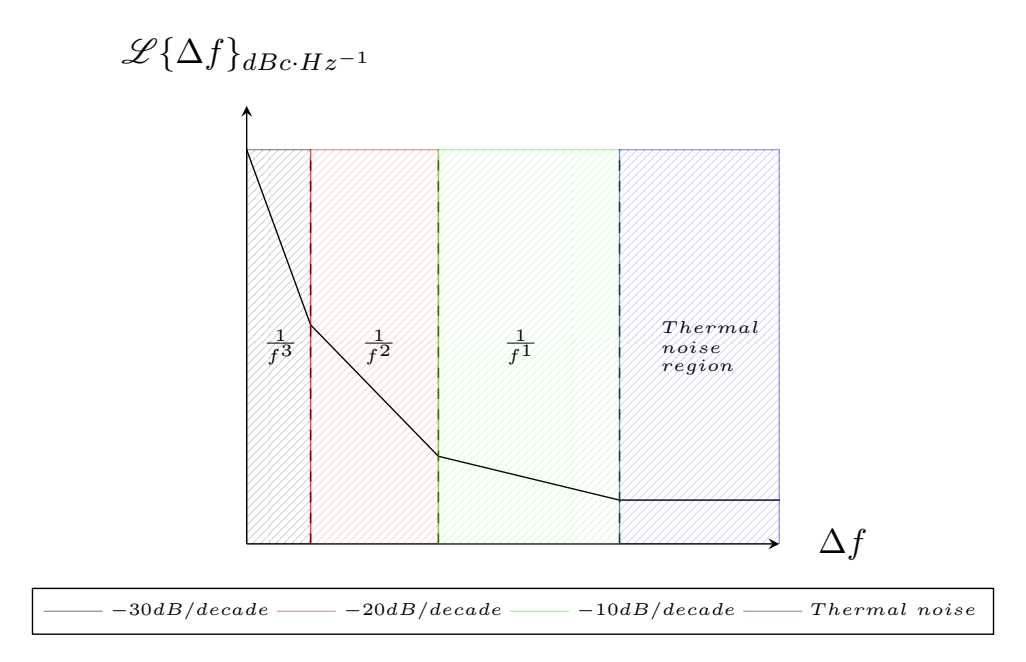


Figure 2.4: Typical oscillator phase noise curve

Phase noise is defined as the ratio of noise power in 1Hz bandwidth at a specified frequency offset  $\Delta f$  from the center frequency to the nominal carrier power, and we note  $\mathcal{L}\{\Delta f\}$  [25]. Phase noise is measured in  $dBc \cdot Hz^{-1}$ . The graph in figure:2.4 represents the noise centered around a carrier frequency with a bandwidth of 1MHz, it contains four regions, the first is the steepest one with a slope of -30dB/decade, the flatness increases to reach the -20dB/decade, then -10dB/decade, lastly the thermal noise floor region. That returns to the fact that noise around the carrier is amplified, and the noise out of the -3dB bandwidth is attenuated.

#### 2.2.1.1 Thermal noise

Thermal noise is a classic type of noise generated by means of Jonson phenomenon which is the random electronic vibrations inside passive and active electronic devices such as: resistors, capacitors, inductors, diodes, transistors, ...ext. The fact that this type of noise is random necessitate a statistical study to characterize it, the probability density function of such signal is said to be a centered Gaussian distribution of variance  $\sigma^2$ . The autocorrelation function is the given by a Dirac distribution of amplitude  $\frac{N_0}{2}W \cdot Hz^{-1}$ , this is explained by the fact that if we took a snapshot of a noise signal their is no way that its samples correlate each other except for a glance of time that is where the Dirac peak appears, in the frequency domain the spectrum of the noise signal is a constant value as the Fourier transform of delta function is a constant.

The minimal thermal noise spectral density generated by a resistively matched system at room temperature is given in [25] by:

$$N = k_B T = 1.38 \times 10^{-23} \times 290 = -174 \ dBm \cdot Hz^{-1} \ [26]$$
 (2.10)

That is the minimal level of noise generated at room temperature in 1Hz bandwidth, this quantity is known as: thermal noise floor.

As mentioned in [25], phase noise component is dominant in thermal noise as amplitude noise is suppressed by the amplitude limiting mechanism, the phase and amplitude noise are assumed to be approximately equal, then the phase noise floor is 3dB below the thermal noise floor:

$$N_{phase} = \frac{N}{2} = N - 3dB = -174 - 3 = -177 \ dBm \cdot Hz^{-1} \ [26]$$
 (2.11)

Finally, the contribution of the active part of the oscillator is taken into account, this amount of phase noise is quantified in the noise factor of the amplifier denoted as F and known as the noise figure when converted to decibels NF, the total thermal phase noise is then given as follows:

$$N_{phase} = \frac{Fk_BT}{2} \Rightarrow N_{phase} = 10log_{10} \left[ \frac{Fk_BT}{2} \right] = -177 + NF_{dB} [26]$$
 (2.12)

As the oscillator output signal has some power level noted as  $P_{in}$  at a specific frequency  $f_o$ , we can reformulate the thermal phase noise expression to take into account the power level of the oscillation signal, we are now speaking of thermal noise floor at a specific frequency with an offset  $\Delta f$  away from  $f_o$ , this quantity is referred to as thermal noise and noted as:

$$\mathcal{L}\{\Delta f\} = \frac{k_B T F}{2P_{in}} [26] \tag{2.13}$$

Equation (2.13) describes the thermal noise at a region far away from the central frequency of oscillations, that explains its simplicity as the noise away from the central frequency is theoretically flat as represented by Leeson's model in figure:2.4, as much as we approach  $f_o$  other noise contributors start to increase the phase noise and become predominate.

### 2.2.1.2 Flicker noise

Flicker noise is characterized by a -10dB/decade slope as represented in figure:2.4, it is said to be situated at the region directly next to the thermal noise region as we are approaching  $f_o$ , its characteristic forms a skirt shape around the central frequency which at the end of it the spectral power density equals to the thermal noise spectral power density. A unifying equation that includes both thermal and flicker noise is given in [25] as follows:

$$\mathcal{L}\{\Delta f\} = \frac{k_B T F}{2P_{in}} \left[ 1 + \frac{f_o}{\Delta f} \right] [26] \tag{2.14}$$

At a far point from the central frequency  $f_o$  we have:

$$\mathcal{L}\{\Delta f\} = \frac{k_B T F}{2P_{in}} \text{ as } \Delta f >> f_o [26]$$
(2.15)

That is the characteristic of the thermal noise given in equation (2.13).

### 2.2.1.3 Oscillator phase noise model

Passing by the history of oscillator characterization, several phase noise models have been introduced. The Leeson's model is a well-known oscillator phase noise model introduced by Professor D.B.Leeson in 1966, this model assumes the linear feedback model for the oscillator as shown in figure:2.5 in addition to four main assumptions [25]:

- Noiseless high gain amplifier with a limit at a level corresponding to the nominal output power.
- The feedback resonator is of bandpass nature centered around the frequency of oscillations and has a Q loaded of  $Q_L$ .
- The noise source represent all noise sources including those introduced by the amplifier and the resonator.
- The amplitude component of the noise is removed by the limiting mechanism of the amplifier, however the phase noise component is stood still.

Then the Leeson's oscillator phase noise model is given by equation (2.16) also known as the Leeson's equation.

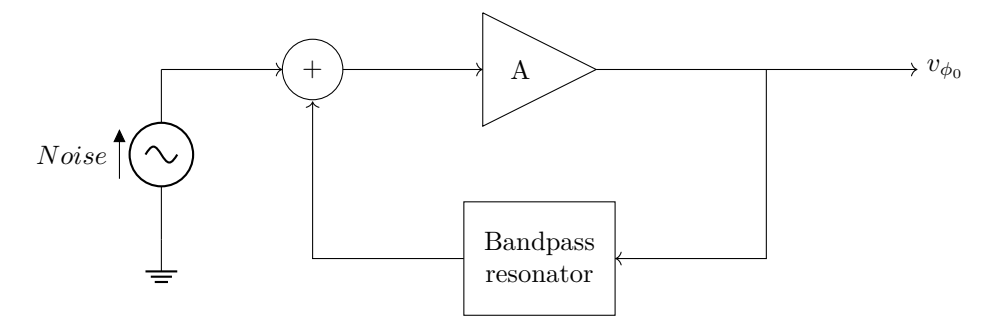


Figure 2.5: Oscillator model assumed in the Leeson's phase noise model

$$\mathscr{L}\{\Delta f\} = \left(\frac{k_B FT}{2P_S}\right) \left[1 + \left(\frac{f_o}{2Q_L \Delta f}\right)^2\right] \left(1 + \frac{f_c}{\Delta f}\right) [26]$$
 (2.16)

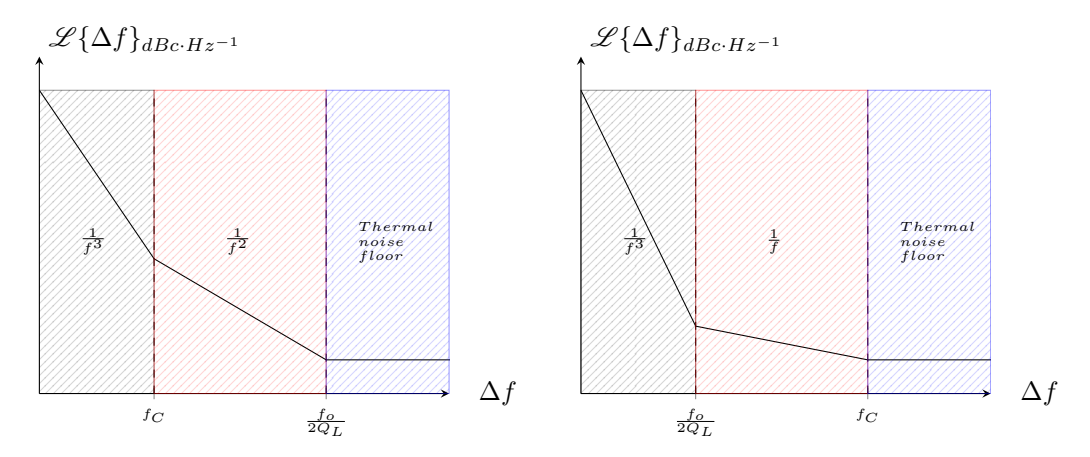
where:

- F: effective noise factor of the amplifier.
- $P_S$ : The power level of the signal at the input of the active element [26].
- $f_o$ : The frequency of oscillations.
- $\Delta f$ : The frequency offset away from the carrier at which phase noise is measured.
- $Q_L$ : The loaded Q factor.
- $f_c$ : The corner frequency between the  $\frac{1}{f^2}$  and the  $\frac{1}{f^3}$  regions.

Due to the fact that the design of oscillator's amplifier is not the same as the design of a simple amplifier, the effective noise factor F are not the same. As mentioned in [25], F is a parameter used to account for the high measured phase noise predicted by Leeson's model.

Writing Leeson's equation in dB will help plotting its asymptotical diagram:

$$\mathcal{L}\{\Delta f\}_{dB} = 10log\left(\frac{k_B T F}{2P_S}\right) + 10log\left[1 + \left(\frac{f_o}{2Q_L \Delta f}\right)^2\right] + 10log\left[1 + \frac{f_c}{\Delta f}\right] [26]$$
(2.17)



- (a) Typical phase noise plot for low Q resonators
- (b) Typical phase noise plot for high Q resonators

Figure 2.6: Typical oscillator phase noise curve

The first term is the thermal noise floor term encountered in section 2.2.1.1, the second term is equivalent to  $20log(\frac{f_o}{2Q_L\Delta f})$  assuming that  $\frac{f_o}{2Q_L\Delta f}>>1$  and it represents the  $\frac{1}{f^2}$  region, the last term which is equivalent

to  $10log(\frac{f_c}{\Delta f})$  as  $\frac{f_c}{\Delta f} >> 1$  represents the  $\frac{1}{f^3}$  region as  $f_c$  is the corner frequency between the  $\frac{1}{f^2}$  and the  $\frac{1}{f^3}$  regions. A plot of the Leeson's model is represented in figure:2.6, as mentioned in [27] the phase noise curve depends of the frequency band the oscillator is designed for, in HF/VHF frequencies we often stumble with high Q resonators and the term  $\frac{f_c}{2Q_L}$  is much smaller than the corner frequency as illustrated in figure:2.6b, however in microwave oscillators, resonators are of a less Q factor, that is the corner frequency is much smaller than the term  $\frac{f_c}{2Q_L}$ , and the phase noise model is the one represented in figure:2.6a.

### 2.2.2 Tuning range

The tuning range of a voltage controlled oscillator is defined as the range of frequencies exhibited at its output, the tuning range is expressed either in terms of bandwidth, that is to mention the first and last frequency at which the VCO oscillates as a bandwidth with the unit Hz, the second way is to express it as a percentage of the central frequency of oscillations, in other words as the ratio of the operation bandwidth of the VCO to the central frequency of oscillations, that is if a VCO is tunable from 1 to 2GHz than in terms of bandwidth the tuning range is 1GHz, and in terms of the ratio of the operation bandwidth to the central frequency the tuning range is:  $\frac{\beta}{f_*} = \frac{1}{1.5} = 0.6666$  that is 66.66% of tuning percentage.

This very tuning range is a key performance parameter when spoken of voltage controlled oscillators specially in broadband applications such as systems relaying on ultra wide band antennas, its restriction is related to the range of instability of the amplifier as well as the tuning range of the varactor diodes used in the resonator, that is to meet the oscillation conditions of the oscillator model, otherwise no oscillation is transferred to the output and the tuning range is not fully achieved.

#### 2.2.2.1 Transfer function of a VCO

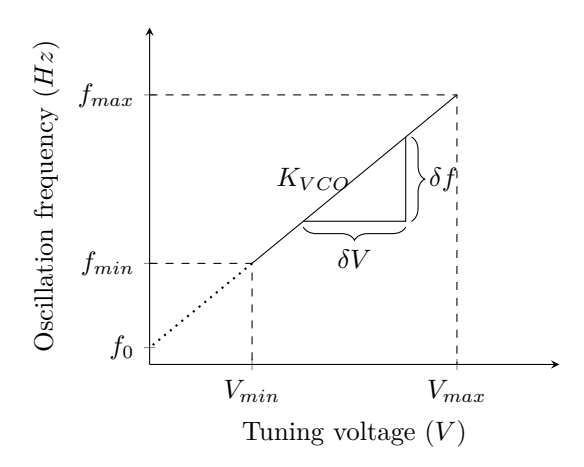


Figure 2.7: Transfer function of a voltage controlled oscillator

A voltage controlled oscillator transfer function figure:2.7, is a function that describes the relation between the tuning voltage and the output frequency of oscillations, that is the transfer from voltage to frequency by means of the VCO. Theoretically the transfer function is typically linear with a slope  $K_{VCO}$  known as tuning sensitivity and the linear equation  $f_{OSC} = K_{VCO} \cdot V + f_0$ , this slope adopts the unit  $MHz \cdot V^{-1}$ , though it depicts the quantity of frequency variation with respect to the variation of tuning voltage.

### 2.2.3 Frequency pushing and pulling

A VCO is a circuit as all electronic circuits, it can not be used independently, it has to be fed by a DC supply voltage which is used to bias the amplifier circuit, as well as to offer power to the output signal. On the other hand, the VCO has to be linked to another microwave stage that is used to exploit its output signal for its intended reasons, otherwise the voltage controlled oscillator is useless.

Since the use of a DC supply voltage is inevitable, the DC bias operation of the amplifier necessitate a fixed voltage which upon the desired instability range is achieved, in other words the characteristics of the amplifier maybe affected by the DC supply voltage variations, these latter can also affect the transistors S parameters [28], which leads to change the instability region of the amplifier, thus the output frequency is drifted from its intended position which is undesired and untolerated in most telecommunications applications, this very phenomenon is known as frequency pushing. On another hand attaching another RF stage to the output of the VCO may affect the phase of its output impedance, that is caused by a load mismatch, hence a change in oscillation frequency occurs, this phenomenon is known as frequency pulling.

As frequency pushing is defined as oscillation frequency change with respect to supply voltage change, it is characterized by the following ratio:  $\frac{\Delta f_{osc}}{\Delta V_{supply}}$ , on the other side frequency pulling is characterized by the ratio:  $\frac{\Delta f_{osc}}{\Delta \Gamma_L}$  since it is due to the load mismatch that leads to change the loads reflection coefficient [23].

### 2.2.4 Harmonic output power

Usually voltage controlled oscillator output signal is not purely sinusoidal, which means that it contains high order harmonics, these harmonics needs to be suppressed so the output would be purely sinusoidal, for that the harmonic output power is a specification used to indicate the power level of high order harmonics with respect to the fundamental frequency power level, a 20dB or more suppression relative to the fundamental according to [29] is typical to achieve a purely sinusoidal output.

### 2.2.5 Power consumption

Concerning DC power supply, the power consumption specification is used as a measure to indicate the amount of DC power drawn by the VCO, it is usually expressed in milliwatts. Its not preferable for a VCO to draw a huge amount of power, that is because of power economy reasons as well as the ease of power providing.

### 2.3 Classification of VCOs

VCOs are classified upon several aspects such as: the manufacturing technology, tuning range, working principle, and output signal type. Through this section of the second chapter we are going to dive into the classification of voltage controlled oscillators upon their topology. Several topologies are going to be explained in the next sections including: LC tank VCOs, ring oscillator VCOs, Colpitts and Hartley VCOs, Dielectric resonator VCOs, and finally Micro Electro Mechanical System MEMS-based VCOs.

### 2.3.1 LC-tank VCOs

An LC tank voltage controlled oscillator inspires its name from the fact that the resonator is an LC feedback network, which is basically an inductor in parallel with a capacitor in case of an oscillator, however in case of a VCO, the capacitors are replaced with an electronic component that the capacity is sensitive to some tuning voltage, that is the varactor diode, the working principle stays the same, and the explanation is going to be upon a conventional LC tank circuit.

The working principle of an LC tank circuit is based in fact on the principle of energy exchange between the capacitor and the inductor, that energy exchange follows a sinusoidal aspect through time that is a pure frequency spectrum that contains only the frequency peak at which the tank oscillates, which is desired in voltage controlled oscillators, up to this theoretical stage their is no problem encountered in the oscillations generation procedure, however in the real world inductors do not behave purely inductive, they have an additional parasitic resistance part, that resistance will cause oscillation damping as depicted in figure:2.8b, their for the tresistance has to be eliminated by means of the active part of the VCO as explained in section 2.1.2, thus steady state oscillations could be generated as illustrated in figure:2.8a.

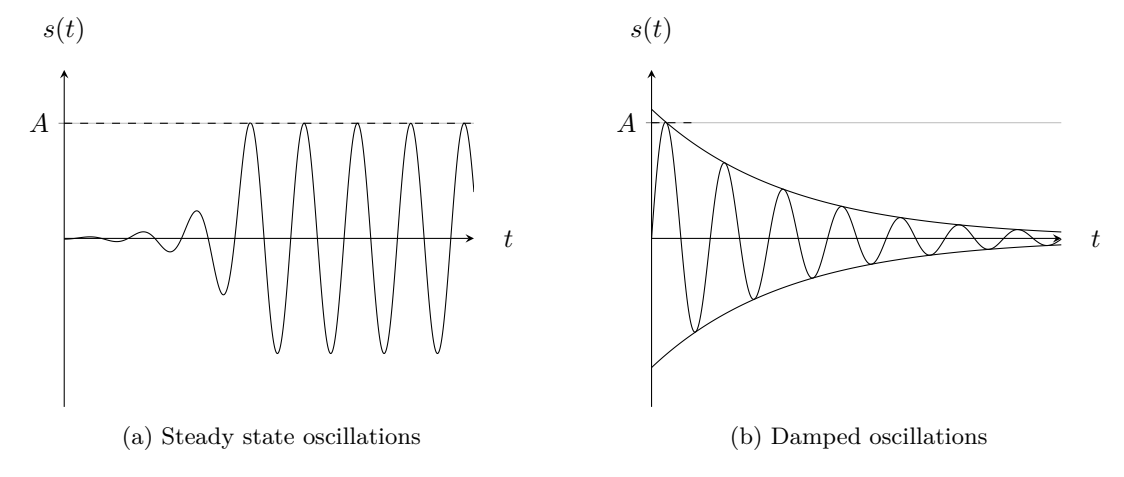


Figure 2.8: Pictorial describes oscillation types generated by means of an LC-tank VCO

#### 2.3.1.1 LC-tank circuit analysis

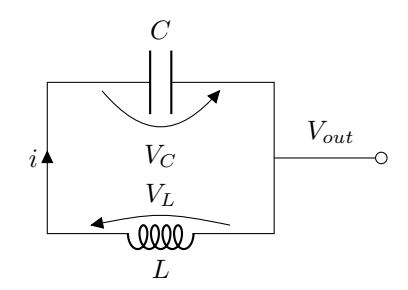


Figure 2.9: Basic LC tank oscillator

Assuming that the capacitor is fully charged, and that the inductor is completely ideal, a proof of the sinusoidal behavior of the output signal  $V_{out}$  of the circuit illustrated in figure:2.9 is going to take place:

Using KVL we can write:

$$V_C + V_L = 0 (2.18)$$

Knowing that:

$$i = C \frac{dV_C}{dt} \tag{2.19}$$

$$V_L = L \frac{di}{dt} \tag{2.20}$$

Equation (2.23) could be written under the form:

$$V_C + L\frac{di}{dt} = 0 \Rightarrow V_C + L\frac{d}{dt} \left[ C\frac{dV_C}{dt} \right] = 0$$
 (2.21)

Then:

$$\frac{d^2V_C}{dt^2} + \frac{1}{LC}V_C = 0 (2.22)$$

Equation (2.22) is a second order differential equation that describes the variations of the capacitor voltage  $V_C$  with respect to time, its solution will give us information about the output signal, assuming at t = 0s,  $V_C = V_0$ , using Laplace transform differentiation and initial value properties equation (2.22) could be solved:

$$\mathcal{L}\left\{\frac{d^2V_C}{dt^2} + \frac{1}{LC}V_C\right\} = \mathcal{L}\{0\}$$
(2.23)

$$s^{2}\mathcal{L}\{V_{C}\} - sV_{0} + \mathcal{L}\{V_{C}\} = 0$$
(2.24)

$$V_C(\omega) = \mathcal{L}\{V_C\} = \frac{sV_0}{\left[s^2 + \frac{1}{LC}\right]}$$
(2.25)

Passing from Laplace to frequency domain by means of the following equation:  $s = \sigma + j\omega$ , which is the case of Fourier transform could be written as:  $s = j\omega$ , equation (2.25) could be written as follows:

$$V_C(\omega) = \frac{j\omega V_0}{\left[\frac{1}{\sqrt{LC}} + \omega\right] \left[\frac{1}{\sqrt{LC}} - \omega\right]}$$
 (2.26)

Observing the denominator of (2.32), two poles could be distinguishable:  $\omega_1 = \frac{1}{\sqrt{LC}}, \omega_2 = -\frac{1}{\sqrt{LC}}$ 

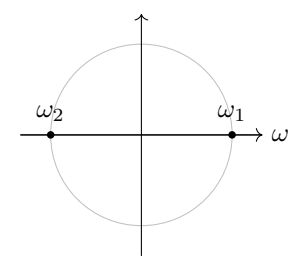


Figure 2.10: Graphical representation of equation (2.26) poles

figure:2.10 could be interpreted as the Fourier transform of a sinusoidal signal, that is as the  $\omega$  domain *i.e.* frequency spectrum is containing two spikes at  $\omega_1$  and  $\omega_2$  for the bilateral representation, however this representation does not describe the real frequency spectrum of such a signal, we relay on the unilateral representation of this frequency spectrum so it could be explained as a real physical signal. A spectrum that contains a unique spike called mathematically a delta function at a specific angular frequency  $\omega_0$ , is undoubtedly a sinusoidal signal with an angular frequency  $\omega_0$ , from this departure idea we can assert that the output signal of an LC tank oscillator is a sinusoidal signal with the frequency  $\omega_0$ .

From the Laplace transform properties listed in [30], it is easy to confirm that the inverse Laplace transform of  $V_C(\omega)$  is a sinusoidal function written as  $cos(\omega_0 t)u(t)$ , that is the causal form of the signal  $cos(\omega_0 t)$ , where  $\omega_0$  is its oscillation angular frequency, hence the output of the LC-tank circuit is sinusoidal. The practical case of this type of oscillators necessitate an active part for the sake of resistance compensation, the overall topology is known as negative resistance oscillator as stated in section 2.1.2.

### 2.3.2 Ring oscillator VCOs

Unlike the previously explained oscillator, ring oscillators does not necessitate an LC-tank feedback network to generate oscillations, thus they are generated by means of a phase inversion mechanism that flips the phase from at the output of each inverter forming a periodic square signal.

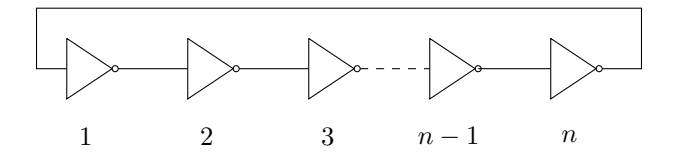


Figure 2.11: A typical ring oscillators

A ring oscillator topology is represented below in figure: 2.11, where the phase shift generated by a single

inverter is 180°, the additional time delay exhibited at the output of each inverter stage is summed up all together and added to the overall phased delay in the loop.

Usually the inverters used in a ring oscillator are identical, therefore the total delay in the loop is equal to  $n(\pi + \phi)$  if their exist n inverters constructing the ring, the total phase shift is composed out of the intrinsic phase inversion feature of the inverter, that is  $\pi$  in addition to the extra time delay converted to a phase delay denoted  $\phi$ . The oscillation condition of a ring oscillator is stated as follows in [31]:

• The number of inverters in a single loop has to be an odd integer.

By consequence the total phase shift is going to be a multiple of  $2\pi$ , and the sum of extra phase shift is going to be equal to  $\pi$ . Under these conditions the signal at the output of the loop will be added in-phase growing up its power and leading towards oscillation.

As stated in [31], the relation of the phase delay  $\phi$  to the extra time delay  $\tau$  is given as:

$$\phi = 2\pi \frac{\tau}{T} [32] \tag{2.27}$$

Equation (2.27) is obtained from the observation of figure: 2.12 and applying the rule of three:

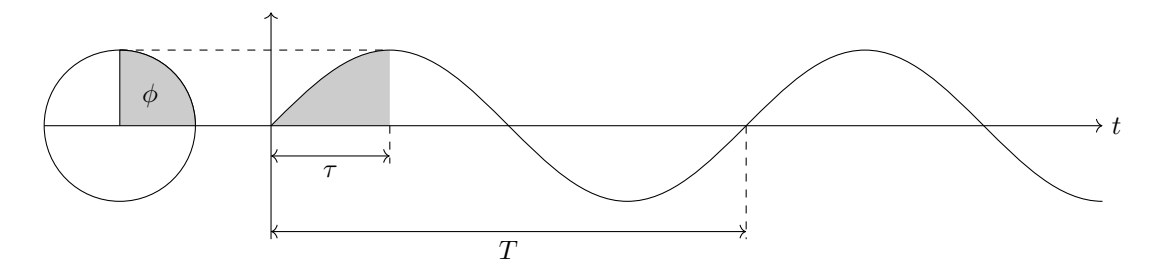


Figure 2.12: Pictorial represents the time to phase delay conversion

As frequency is the inverse of the period, we can write:

$$f_0 = \frac{1}{T} = \frac{\phi}{2\pi\tau} \ [32] \tag{2.28}$$

Since  $n\phi = \pi$ ,  $\phi = \frac{\pi}{n}$  Therefore:

$$f_0 = \frac{\pi}{2n\pi\tau} \Rightarrow f_0 = \frac{1}{2n\tau} [32]$$
 (2.29)

Where:

- $f_0$  is the ring oscillator frequency of oscillation.
- *n* is the number of inverters in the ring.
- $\tau$  is the extra time delay at the output of each inverter.

In most microwave applications n is kept as small as possible to maximize the oscillation frequency, however the real maximization of  $f_0$  relays on minimizing the extra time delay  $\tau$ . Ring oscillators are mostly used inside locked systems such as phase locked loops due to the fact that their phase noise is reduced while the ring oscillator is locked by a source signal.

### 2.3.3 Colpitts and Hartley VCOs

Another type of oscillators is to be discussed, that is the Colpitt's and Hartley oscillators. These types of oscillators are based upon the LC-tank resonators, their topology includes a transistor amplifier based on BJT's or Field Effect Transistor's FET's in microwave applications. As shown in figure:2.13, the transistor  $Q_1$  is polarized via a resistive bridge formed by  $R_1$  and  $R_2$ , the emitter resistance  $R_E$  is used to prevent the transistor from drifting from its Q point, the inductor  $L_{DC}$  is used to isolate the amplifier oscillations from DC feed voltage supply, its second purpose is to generate negative resistance at the base of  $Q_1$  [23] for the sake of resonator resistance compensation, thus achieving instability. While  $R_E$  is used for its purpose in DC mode, it has a side effect in AC mode which is to decrease the voltage gain of the amplifier, therefore the shorting capacitor  $C_E$  is used to short it out in AC mode. The main difference between Colpitt's and Hartley oscillators lays in the feedback network, they both use a "II" feedback however they differ the components used for construction as shown in figure:2.13a and 2.13b. As stated in [32], for a proper feedback in Hartley's topology  $L_1 > L_2$ , the gain condition have to be also satisfied under the form:

$$h_{21} = \beta \ge \Delta h \frac{L_1}{L_2} [33] \tag{2.30}$$

Where:

- $\beta$ : current gain of the transistor.
- $\Delta h$  determinant of the hybrid matrix of the transistor.

$$h = \begin{bmatrix} h_{11} & h_{12} \\ h_{21} & h_{22} \end{bmatrix} \Rightarrow \Delta h = h_{11}h_2 - h_{12}h_{21} [33]$$
 (2.31)

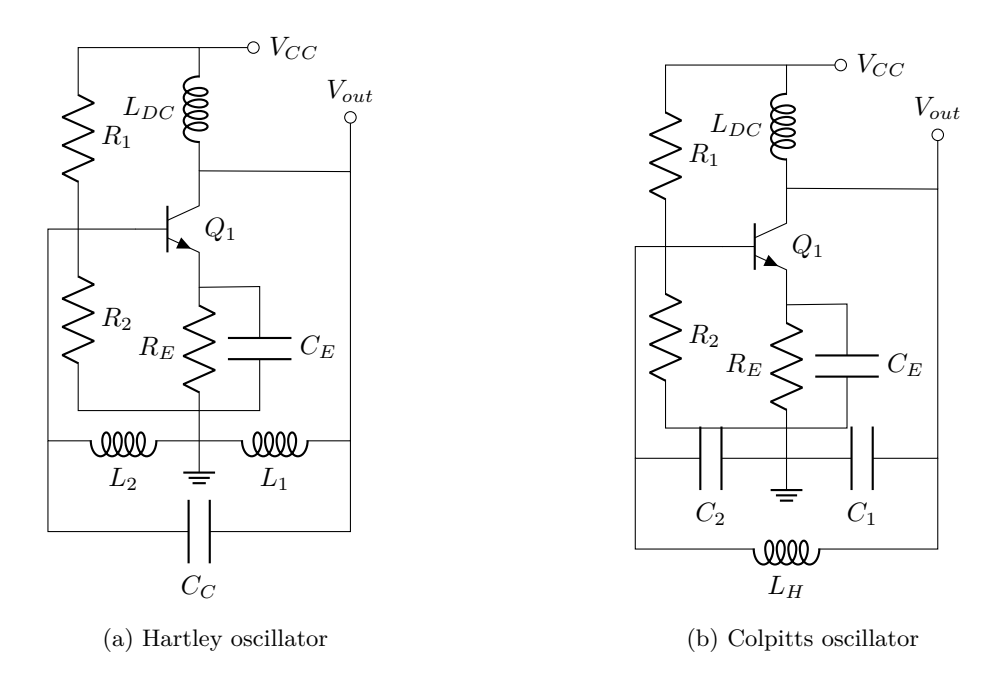


Figure 2.13: Hartley and colpitts oscillators

The oscillation frequency of Colpitt's and Hartley oscillators is give by the expression:

$$f_{osc} = \frac{1}{2\pi\sqrt{LC}} [33]$$
 (2.32)

Where For  $C_C$  and  $L_H$  are given by:

$$C_C = \frac{C_1 C_2}{C_1 + C_2} L_H = L_1 + L_2 [33]$$
(2.33)

### 2.3.4 Dielectric Resonator Oscillators DROs

As seen in the previously explained oscillators, all the resonators are made out of conductor materials combined with lumped electronic components, as the quality factor is inversely proportional to the real part of the resonators impedance, it will be decreased by means of the conductors used to manufacture the resonator. Microwave engineers thought of a solution that meets the high quality factor characteristic of the resonator, therefore dielectric resonators where found to replace conductor resonators in some radio frequency applications such as navigation and electronic warfare. A real world model of a dielectric resonator oscillator that delivers a 4.5GHz frequency output is shown in figure:2.14 from [33].

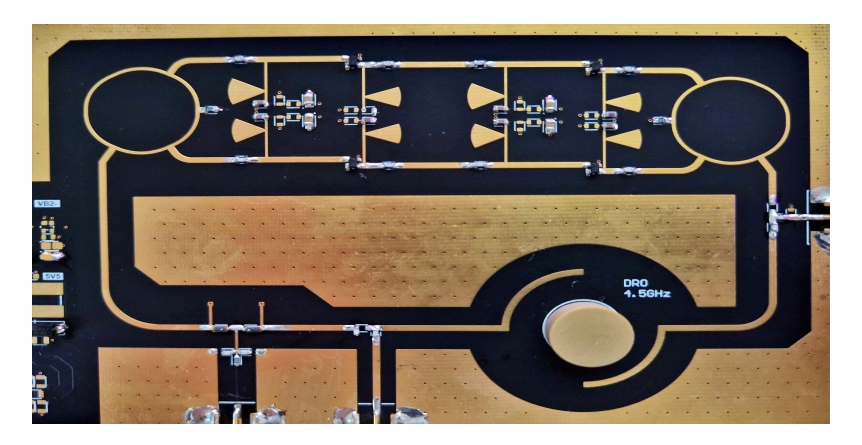


Figure 2.14: Dielectric resonator oscillator

According to [34], the dielectric resonator dimensions are typically given as follows: the height is 35% to 50% of its diameter.

#### 2.3.4.1 Resonant frequency

The oscillation frequency of a DR is inversely proportional to its volume, and its given in [34] by the following expression:

$$f_R = \frac{34}{D\sqrt{\epsilon_r}} \left[ \frac{D}{h} + 6.9 \right] [35] \tag{2.34}$$

Where:

- D: the resonator diameter.
- $\epsilon_r$ : the relative permittivity of the dielectric.
- h: height of the dielectric.

It is cited in [34] that the tuning range of a DRO is somewhat narrow, this is due to the fact that frequency shifting is inversely proportional to the unloaded Q factor of the resonator, where 20% frequency shift decreases the quality factor by 50% which is significant. That narrows down the field of exploitation of dielectric resonator oscillators down to applications with narrow bandwidth such as radar systems.

### 2.3.4.2 Dielectric resonator unloaded Q factor $Q_U$

The  $Q_U$  factor is the quality factor determined with the resonator unloaded, that is the quality factor of the resonator purely. This parameter is of great interest as Dielectric Resonator's DR's are devices said to be of high quality factor comparing to other resonator technologies.

The expression of  $Q_U$  of a cylindrical hollow dielectric resonator as shown in figure:2.15 is given by:

$$Q_U = Q_0 \left[1 - \gamma e^{\frac{\gamma}{2} \frac{D_{cavity}}{D}}\right] [35]$$
 (2.35)

Where:

- $Q_0$ : Unperturbed unloaded Q factor.
- $\gamma$ :  $\sqrt[3]{\epsilon_r} 1$ .
- $D_{cavity}$ : diameter of the cavity.
- D: diameter of the dielectric.

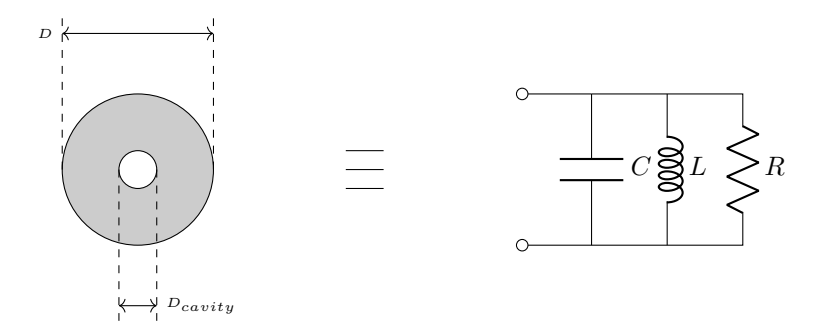


Figure 2.15: Dielectric resonator equivalent circuit

#### 2.3.4.3 Dielectric resonator coupling

A dielectric resonator is usually coupled to a circuit via microstrip transmission lines, the coupling is done as the field lines of the resonator are aligned with those of the microstrip TL's. The fact that plays a crucial role at this stage is the dimension between the centre of the resonator and the close side of the transmission line, where maximum coupling is achieved when this later is less than the radius of DR.

Coupling is quantized by a coupling coefficient denoted as k given by:

$$k = \frac{S_{11}}{S_{21}} [35] (2.36)$$

An analytical model of the coupling coefficient is given in [34] knowing the lowest value of  $S_{21}$  at the resonant frequency, hence:

$$k = 10^{\frac{-S_{21(dB)}}{20}} - 1 [35] (2.37)$$

Usually the transmission coefficient  $S_{21}$  is used in this case to determine the loaded and unloaded quality factors, where they equal to the bandwidth of the response divided by the resonant frequency with xdB below the 0dB for  $Q_L$  and xdB above the lowest  $S_{21}$  value for  $Q_U$  as shown in figure:2.16, where x is a quantity given in decibels state by a formula in [35]:

$$\begin{cases} x(dB) = 3 - 10log_{10} \left[ 1 + 10^{-0.1L_o} \right] \\ L_o(dB) = 10log_{10}(S_{21}) \end{cases}$$
 [35]

At the resonant frequency  $S_{21}$  is very low which makes x converge towards 3dB. Knowing x, k, and  $Q_U$  leads to model the dielectric resonator by means of lumped passive components where the expressions are given in [34] as:

$$R = 2Z_0 k [35] (2.39)$$

$$C = \frac{1}{(2\pi f_R)^2 L} [35] \tag{2.40}$$

$$L = \frac{R}{2\pi f_R Q_U} [35] (2.41)$$

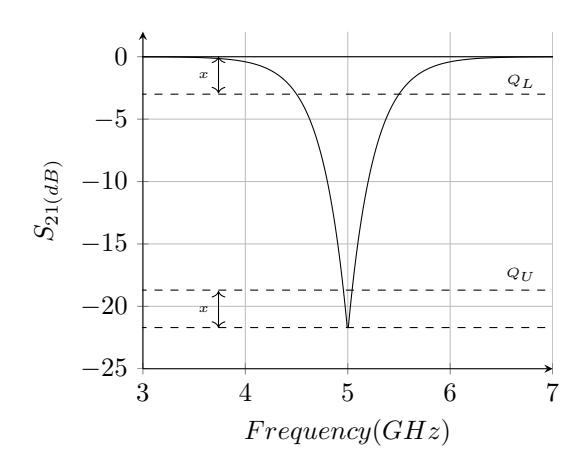


Figure 2.16:  $S_{21}$  parameter of a dielectric resonator

#### 2.3.5 MEMS-based VCOs

The term MEMS stand for Micro Electro Mechanical System, a MEM oscillator is a combination of a micro mechanical system and an electrical system, when a voltage is applied to that micro mechanical system it will vibrate at a specific frequency, the mechanical oscillations are then converted into an electrical signal via a transducer, hence electrical oscillations are generated out of mechanical oscillations. MEMS oscillators are usually made out of polysilicon glass, aluminium or silicon itself [36], they are known for their low power consumption, miniature size, and enhanced reliability [37]. According to [37], the overall topology of a MEMS based oscillator necessitate the existence of three main parts:

- Micro-scale resonator: That is the part responsible of generating oscillations.
- Electronic control circuitry: A driving and control circuit is needed to control the vibrations of the resonator.
- Feedback mechanism: Like all oscillators a feedback mechanism is needed to bring back energy from the output, that is to sustain oscillations.

### 2.3.5.1 Basic principle of operation of a MEMS oscillator

For the sake of simplicity, the system explained is [36] is taken as a reference, the system is an equivalent to a real MEMS resonator though it consists of a mass spring mechanical oscillator and a transducer capacitor.

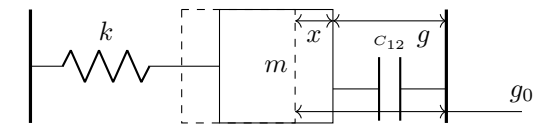


Figure 2.17: Equivalent MEMS oscillator

The angular frequency of the mass spring mechanism is given by:

$$\omega_m = \sqrt{\frac{k}{m}} \ [37] \tag{2.42}$$

The electrical capacitance of the transducer is:

$$C_{12} = \frac{A\epsilon_0}{q} [37] \tag{2.43}$$

Where:

- A: is the area of the gap after displacement.
- $\epsilon_0$ : is the vacuum permittivity.
- g: is the gap.

When a voltage is applied to the resonator a force  $\vec{F}$  is generated, as a consequence the mechanical system will be moved by a linear amount x:

$$F = QE = C_{12} \frac{V^2}{g} = A\epsilon_0 \frac{V^2}{g^2} [37]$$
 (2.44)

For small voltage variations, the force varies as follows:

$$\frac{\delta F}{\delta V} = \frac{\delta}{\delta V} \left[ A \epsilon_0 \frac{V^2}{q^2} \right] = 2A \epsilon_0 \frac{V_0}{q^2} \delta V$$
 [37]

The mass m is then moved by the amount x that equals to:

$$\delta x = \eta_d \frac{\delta F}{k} [37] \tag{2.46}$$

Where  $\eta_d$  is the efficiency coefficient of the displacement power.

#### 2.3.5.2 MEMS oscillator figure of merit

Knowing the amount of displacement generated by the force  $\vec{F}$ , leads us to write the expression of the mechanical energy stored in the system:

$$\delta E_m = \frac{1}{2} \delta F \delta x = \frac{\eta_d \delta F^2}{2k} = \frac{2\eta_d A^2 \epsilon_0^2 V_0^2}{k q^4} \delta V^2 [37]$$
 (2.47)

Where  $C_m = \frac{4\eta_d A^2 \epsilon_0^2 V_0^2}{kq^4}$  is the motional capacitor, that is used to define the figure of merit of the oscillator.

$$M_0 = \frac{QC_m}{C_{12}} = \frac{4\eta_d Q A \epsilon_0 V_0^2}{m\omega_m^2 g^3} [37]$$
 (2.48)

In conclusion MEMS based oscillators operate by transducing mechanical into electrical vibrations by applying a DC voltage upon a mechanical structure that serves as a resonator, they are characterized by their resonant frequency as well as their figure of merit which is defined in equation (2.48) for oscillators adaptable to the model represented in figure: 2.17.

After delving through the various VCO technologies working principles, an idea upon which technology is used to construct the proposed VCO is constructed, thus in the next chapter a circuit design and simulation are going to take place.

## 2.3.6 Quartz oscillators

A quartz crystal oscillator operates based on the piezoelectric effect as stated in [38], where a quartz crystal mechanically vibrates when subjected to an alternating electric field, and conversely, generates an electric signal when mechanically stressed. When integrated into an amplifier feedback loop, the quartz crystal acts as a highly selective resonant element. Due to its mechanical resonance, the crystal provides a narrow frequency band where the phase shift and gain conditions required for oscillation (as defined by the Barkhausen criterion) are naturally satisfied. The equivalent electrical model of a quartz crystal includes a motional inductance (L), motional capacitance (C), and motional resistance (R), in series, all shunted by a static capacitance (C). This configuration ensures the oscillator stabilizes at or near the crystal's natural mechanical resonance, resulting in highly stable and low-noise frequency generation.

# 2.3.6.1 Oscillation frequency

The primary oscillation frequency of a quartz crystal is determined by its physical dimensions, cut angle, and mode of vibration. It corresponds to either the series resonant frequency (where the motional impedance is minimized) or the parallel resonant frequency (where the crystal acts as a high-impedance tank circuit due to the interaction of C and C). These are given approximately by: Series resonant frequency:

$$f_s = \frac{1}{2\pi\sqrt{L_1C_1}} \ [38] \tag{2.49}$$

Parallel resonant frequency:

$$f_p = f - s\left(1 + \frac{C_1}{2C_0}\right) [38]$$
 (2.50)

# Chapter 3

# Design and Simulation of the Proposed VCO

In the previous chapter an overview upon VCO working principle, their key performance parameters, and a brief classification of VCOs were mentioned, the latter helps to construct an idea upon the realm of voltage controlled oscillators, consequently a one may select the intended VCO specifications which permits leaping from the knowledge gathering phase to the design and simulation phase.

Through this chapter named as: "Design and Simulation of the Proposed VCO", the reader will go through the experience of RF and microwave circuit design from the first to the last step as follows:

- Specification setting.
- Topology and and component selection.
- Schematic simulation using Computer Aided Design CAD tools such as ADS.
- Performance evaluation by analyzing simulation results.

# 3.1 Specification and design requirements

The proposed VCO is based on microstrip line technology as the one mentioned in section:1.4.2, its specifications are mentioned in table:3.1, these specifications represent the intended goal from this voltage controlled oscillator.

Tuning range	[0.9 - 1.6]GHz
Output power	> 0dBm
Technology	Microstrip
Supply voltage	< 10V
Phase noise	<-120dBc/Hz @ $1MHz$ $offset$
Figure of merit	< -160dBc/Hz
Tuning voltage	[0 - 30]V
loop gain	≥ 1

Table 3.1: Specifications of the proposed VCO

To achieve this VCO specifications some critical requirements must be respected, as the design is going to be based on an RF BJT transistor amplifier, the selected transistors must go far beyond the upper frequency limit of the tuning range, that is 1.6GHz, this is considered to prevent unstable behavior at the limit of the operating frequency of the active device. In order to generate oscillations at the intended range, the varactor diodes used in the resonator must be carefully selected, that is because the oscillation frequency is related to their

capacitance which makes them the key component that enables frequency control in a VCO, this is required to prevent frequency from drifting toward undesired ranges where oscillation conditions are not verified.

From transmission lines point of view, the dimensions of microstrip lines must be tuned to a point where they port a transparent effect on the circuit, another consideration is that the smallest microstrip gap width allowed is 0.2mm, beyond this width no gap is going to be printed using our printing technology.

# 3.2 Simulation tools and methodologies: ADS

ADS also known as Advanced Design System is an electronic automation design software, a premier high-frequency and high speed design platform developed by PathWave design a devision of Keysight technologies, its initial release was in 1985 under the name Microwave Design System MDS, the software could be installed on both Linux and windows operating systems. ADS is mainly used for electronic circuit simulation, precisely to design RF electronic products such as circuits used in mobile phones, wireless networks, satellite communications, radar systems, and high speed data links. ADS is a powerful design and simulation tool as it is capable of supporting every step of the design process:

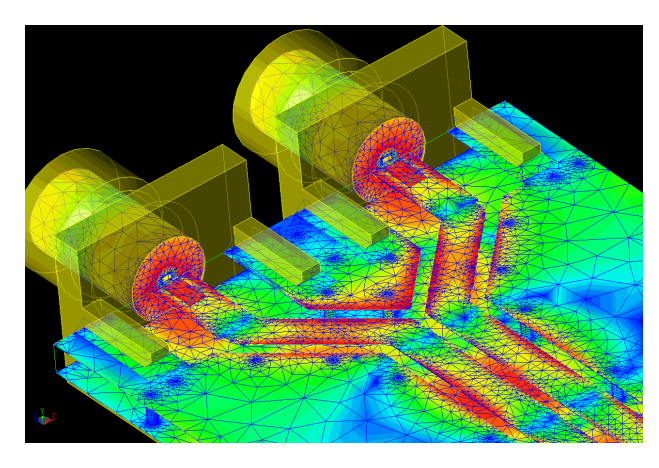


Figure 3.1: EMpro environment

schematic design, layout generation, frequency and time domain simulation and also electromagnetic simulation using finite element method or momentum method as shown in figures:3.1, 3.2 from [39] [40] respectively, another key feature of this software is the cosimulation simulation, that is described as a type of simulation where Electro Magnetic EM simulated components are combined with circuit simulated components in order to perform a hybrid simulation, the latter is very close to reality as microwave structures are simulated using an EM simulator while lumped components preserve their characteristics, therefore this type of simulation is similar to real circuit measurements. A point that is counted as an advantage for ADS is its user-friendly interface as well as its real components data base, that means if a designer tries to simulate a circuit then real components are used in the software, the models are usually provided by the manufacturers under the form of design kits compatible with ADS.

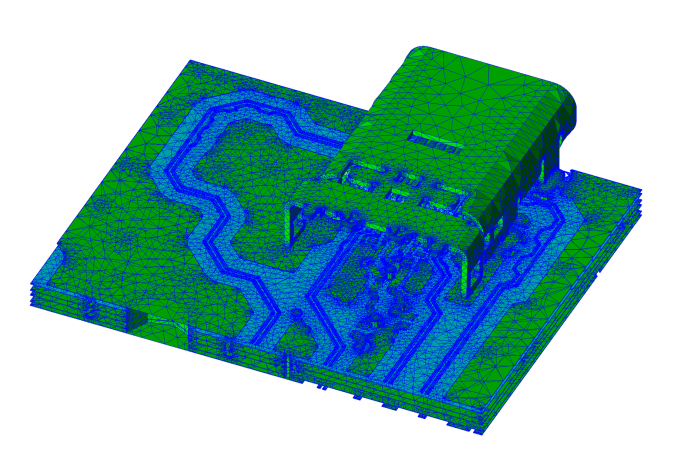


Figure 3.2: FEM simulator

This software is capable of performing several kinds of simulations including:

- Transient
- DC
- AC
- Harmonic balance
- S parameter
- X parameter
- Circuit budget

- Large signal S parameter
- Gain compression
- Circuit envelope
- Load pull
- Channel
- Batch
- DDR

# 3.3 Selection of topology and components

A traditional voltage controlled oscillator is a device constructed from an amplifier and a feedback loop, however by research advancements new topologies were proposed such as: cross coupled VCOs, push-push VCOs, differential cross coupled VCOs, ...ext. All of these topologies possess advantages and inconvinients, which means that the selection of one of them will be based upon which characteristic is elected to be satisfied the most by the designers, this may lead to create a compromise between the characteristics, however it could be handled using tuning.

# 3.3.1 Amplifier design

Our strategy is to capture the hardest parameter to achieve from table:3.1, then a topology that promises achieving the latter is selected, the overall circuit is then tuned to reach other specifications. In VCOs the most important key parameter is phase noise as it serves the purity of the output spectrum, a topology is then proposed to achieve low phase noise levels at 1MHz offset from the frequency of oscillations over the whole frequency band, that is the push push BJT voltage controlled oscillator. The proposed topology decreases the level of undesired signals common to both of its inputs, this feature is characterized by a parameter known as: Common Mode Rejection Ratio denoted a CMRR, this parameter is defined as the ratio of the differential gain of the amplifier to the common mode gain [41]. The ideal case of a push push amplifier is described by a null common mode gain, by consequence an infinite CMRR, however in the practical case  $A_c \to 0$ ,  $A_d >>$  then:  $CMRR \to \infty$ .

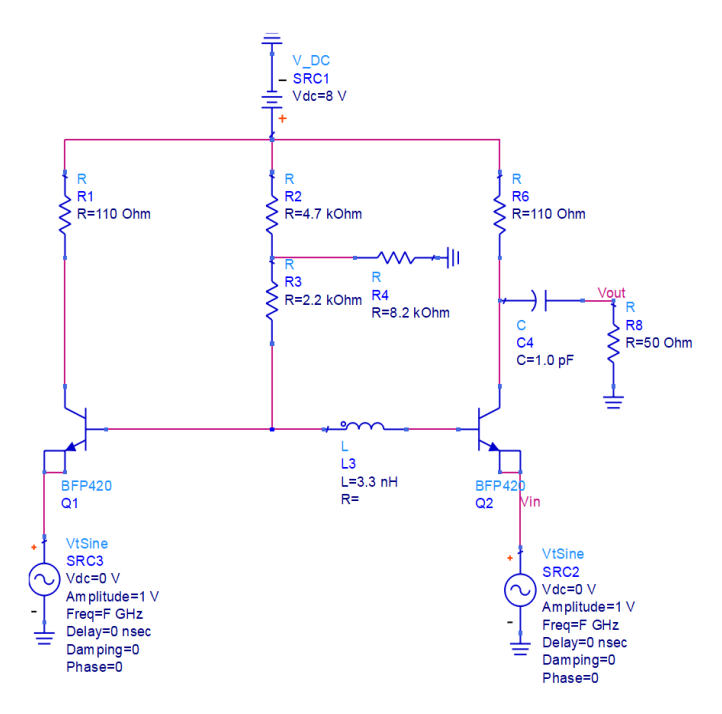
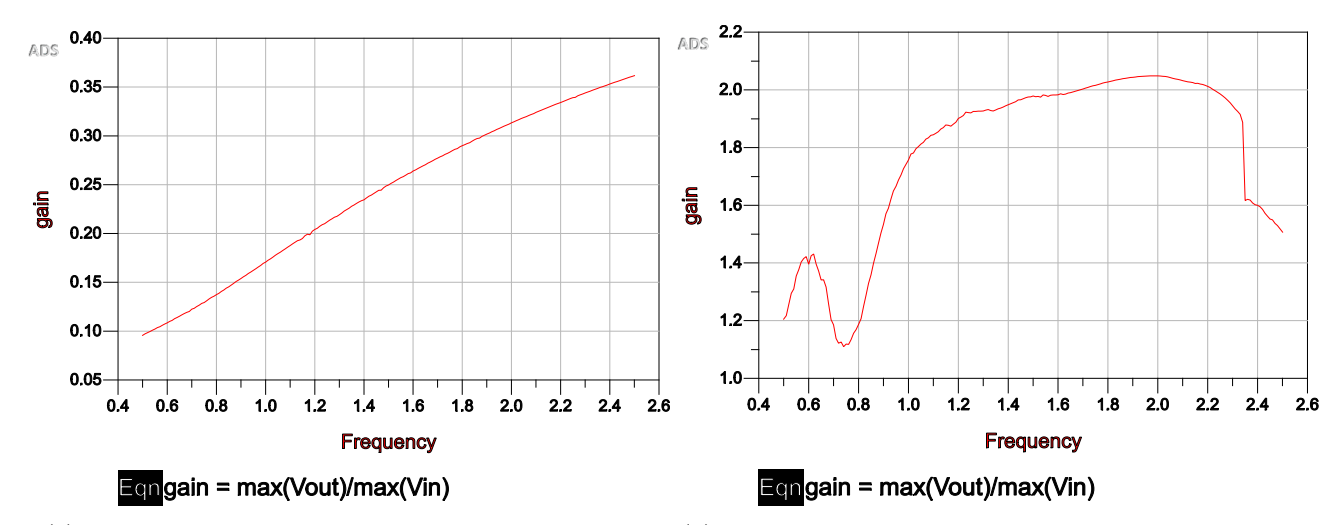


Figure 3.3: Proposed push push amplifier

Before diving through simulation results discussion of the circuit in figure:3.3, an explanation of circuit it self must take place. The circuit consists of a pair of base to base connected bipolar junction transistors, silicon based Negative Positive Negative NPN BJT's such as BFP420 [42] are known for their low cost and proven reliability as they are used in Ultra High Frequency UHF and microwave bands [43], nevertheless it is mentioned in [42] that this device is used for radio frequency oscillators, therefore the BFP420 is selected as the transistor used to construct the push push amplifier, the footprint for this device is the SOT-343 [42]. The resistors  $R_2$ ,  $R_3$  and  $R_4$  are polarization resistors as they provide the adequate voltage to the base so the  $V_{BE}$  threshold is achieved in both  $Q_1$  and  $Q_2$  otherwise both devices are in the off state. the inductor  $L_3$  is a reactive element used to generate negative resistance at the emitter of the active devices as explained in [23].



(a) Common mode gain curve with respect to frequency. (b) Differential mode gain curve with respect to frequency.

Figure 3.4: Simulated gain modes variations with respect to frequency.

 $C_4$  is a DC blocking capacitor, and  $R_8$  is a 50 $\Omega$  resistor used to extract the output signal, two signal sources SRC2 and SRC3 are used to simulate the common mode and differential gain of this amplifier, the configuration in figure:3.3 is used to simulate the common mode gain, the same is used to simulate the differential gain with SRC3 shorted. The sources are said to be similar as they are ideal sources inside the simulation software.

As illustrated in figure:3.4, the common mode gain tend toward zero, hence at 1.6GHz the common mode rejection ratio is:  $CMRR = \frac{A_d}{A_c} = \frac{1.982}{0.264} = 7.5$  That means that common mode signals are seven times week than differential mode signals, assuming noise as a common mode signal phase noise could be enhanced using this amplifier topology. Despite that, the CMRR could be improved further by increasing the differential gain, however this is not very important in this case as this amplifier is going to server as the active part of a voltage controlled oscillator, from another point of view improving the CMRR by increasing the amplifier gain could lead to design a high attenuation resonator to suppress the gain effect ported by the active device, otherwise oscillation conditions are not satisfied, hence no oscillations are produced.

#### 3.3.2 Resonator design

Moving now to the resonator, similarly to an LC cross coupled VCO where the resonator is installed between the collectors, in this design the resonator will be installed between the emitters, the latter is constructed from an inductor and two capacitors, along with a parallel resistance, the role of the capacitors along with the inductor is to provide oscillations, however the resistance is used to control the attenuation level of the resonator.

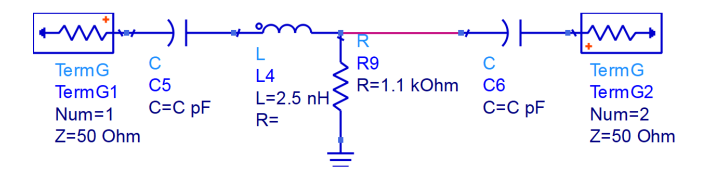


Figure 3.5: Resonator circuit

Figure:3.5 shows the circuit of the proposed resonator, the resonant frequencies of this circuit are shown in figure:3.6 where each valley of an S(1,1) curve is associated with a resonant frequency of a given capacitance value, the capacitance is swept from [5-19]pF so it meets the adequate frequency tuning band. The resonant frequency of the circuit shown in 3.5 does not really equal to the oscillation frequency as other capacitors will be included in the complete VCO circuit, that might cause some frequency drifting which must be minimized. In order to make frequency sweep available the capacitors  $C_5$  and  $C_6$  are replaced by varactor diodes of adequate capacitance values, the varactores used are BB135 varactor diodes, this diode is a UHF variable capacitance

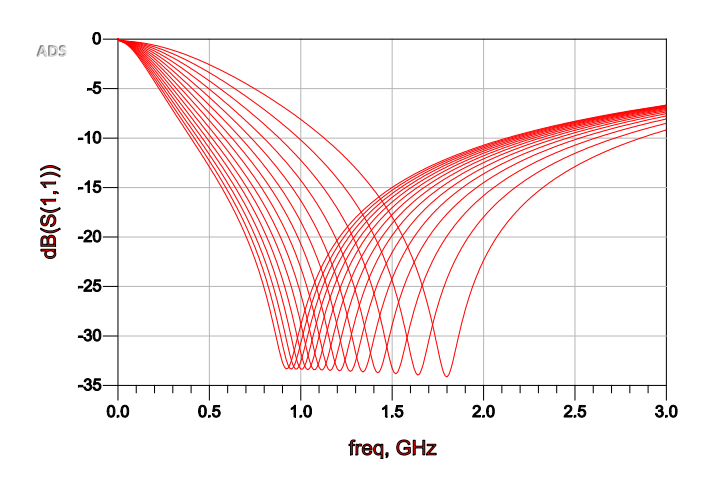


Figure 3.6: Frequency response of the resonator using lumped capacitors

surface mount diode that could achieve 1.7pF at 30V of reverse bias voltage, the footprint used for these diodes is the SOD-323 according to [44].

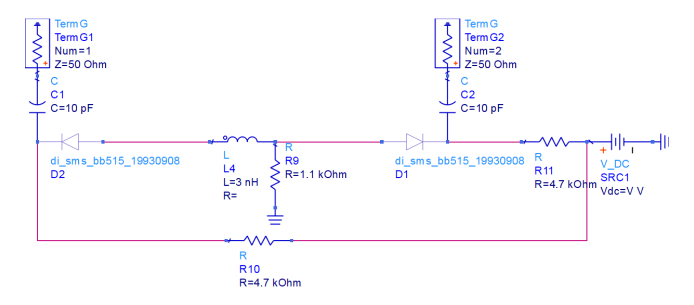


Figure 3.7: Varactor diodes resonator.

The circuit in figure:3.7 shows the variable capacitance version of the resonator, as it is seen the capacitors were replaced by BB515 diodes, the reason why this component is used instead of the BB135 is because its unavailable in ADS simulation software, however the BB515 serves as its equivalent, the reverse bias of both diodes is provided by SRC1 via resistors  $R_{10}$  and  $R_{11}$ , the capacitors C1 and C2 are DC blocking capacitors used to block DC bias voltage from leaking to the terminals of the resonator.

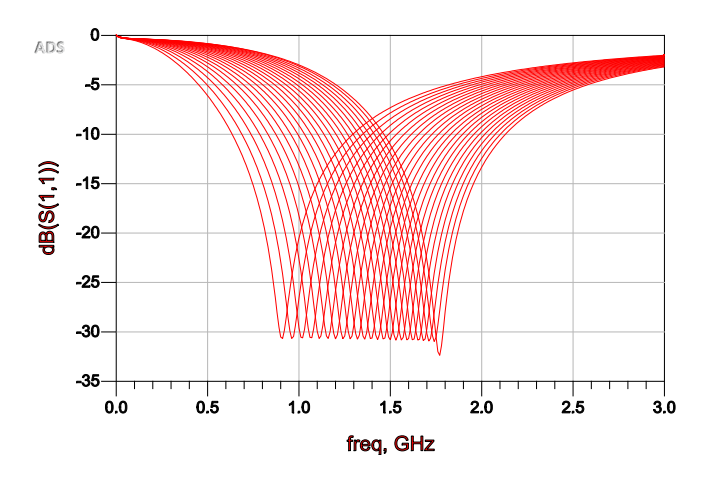


Figure 3.8: Frequency response of the resonator using varactor diodes

As depicted in figure: 3.8 the frequency response of the resonator with variable capacitance diodes is similar to the frequency response of the lumped components resonator, that qualifies the BB135 to be the diode used to construct the proposed voltage controlled oscillator, the tuning voltage was varied from 0V up to 22V.

These are the two critical components which must be well explained, which are the BB135 diode and the BFP420 transistor, other passive components are used either for polarization, impedance matching, negative

resistance generation, or for blocking DC energy from leaking to RF blocks, the only thing that must be mentioned is that all components used in this VCO are surface mount components due to the small size of the overall circuit.

# 3.4 Circuit design and modeling

# 3.4.1 Stability of the amplifier:

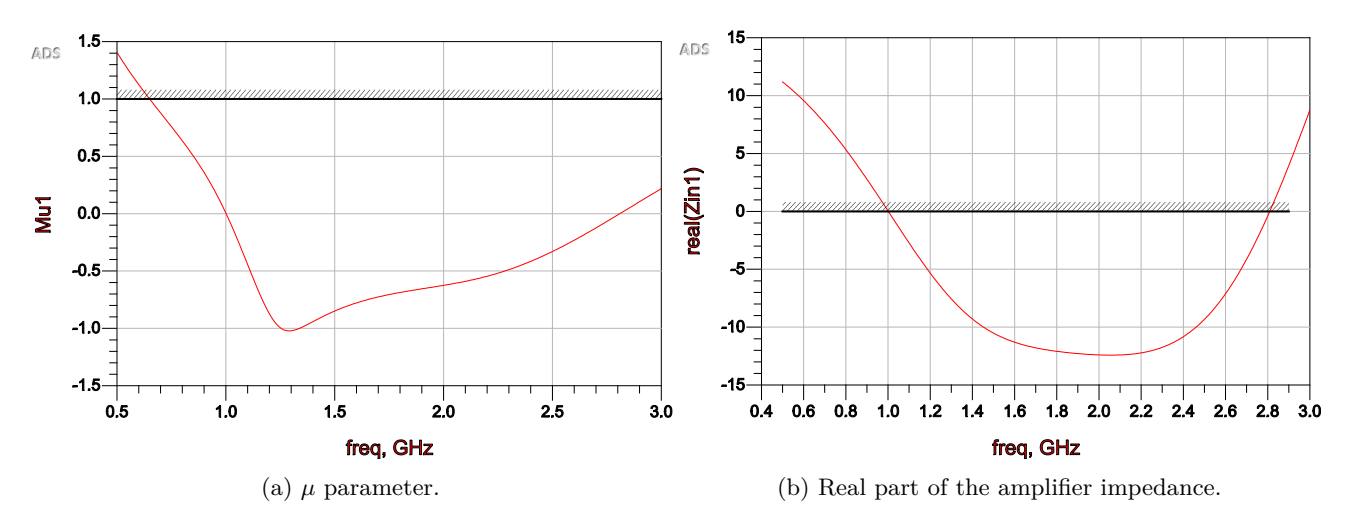


Figure 3.9: Push push amplifier stability.

Before proceeding with the design of the VCO circuit, the stability of the amplifier must be studied, otherwise if it is stable at some frequencies inside the tuning range, no oscillations are produced as the instability of the active device is the key to generate oscillations. The stability study of a microwave device relays on checking Rollet's conditions as mentioned in [20], however in the same reference it is mentioned that stability could be verified using another recent parameter known as  $\mu$ , this parameter is the one used in ADS simulation software as mentioned in [45], for any microwave circuit if  $\mu$  is greater than unity the circuit is stable, otherwise the circuit is considered unstable, for our voltage controlled oscillator unconditional instability must be verified over the frequency tuning band to insure oscillations without discontinuities. As seen in figure:3.9a,  $\mu$  is below unity from around 0.7GHz up to beyond 3GHz, therefore unconditional instability is guaranteed along the frequency tuning range, as the latter is included inside the frequency band where  $\mu < 1$ . Figure:3.9b depicts the negative real part the amplifier impedance generated at its emitters in this case.

# 3.4.2 Circuit design

The overall circuit design consists of connecting the amplifier and the resonator in a loop, as shown in figure:3.10 the design of the VCO included also some additional components and devices such as capacitors  $C_{25}$ ,  $C_{26}$ , their role is to make a matching interface between the amplifier and the resonator, they also serve as DC blocking capacitors. The butterfly structure before the output of the VCO is a butterfly low pass filter used to isolate the fundamental frequency, its cutoff frequency is 2GHz, and it has a high attenuation at the rejected band to make sure that all harmonics are below the -20dB power level as mentioned in section: 2.2.4, that is to suppress their contribution to the output signal, hence a pure sinusoidal signal is passed to the output. The capacitor  $C_{27}$  proceeding the filter is used to block DC from leaking to the output.

The transformer  $TF_1$  is used to probe the oscillator while operating without disturbing its common behavior, the purpose of using it is to verify oscillation conditions of a negative resistance oscillator by means of an S parameter setup used to measure the impedance between the active device and the feedback loop, the conditions over the whole bandwidth are said be:

$$\Re\{Z\} < 0, \ \Im\{Z\} = 0 \tag{3.1}$$

Oscport2 is a device driven by means of a harmonic balance simulation controller, the device is used with VCOs based on differential amplifiers to check for loop gain and tries to bring it to unity, if it is the case a steady-state of oscillations is detected, otherwise *i.e.* loop  $gain \neq 1$  the simulation diverges and no steady-state is detected.

From simulation point of view both oscillation conditions mentioned in sections: 2.1.1 and 2.1.2 are verified by means of the transformer setup and the Oscport2. The stubs TL175 and TL3 are used in exchange of using lumped SMD inductors as their values are relatively low, that permits their printing as the stub dimensions and the inductance are related directly using the following equation given in [46]:

$$L = 0.0002l \left[ ln \left( \frac{4l}{b} \right) + 0.0224 \left( \frac{b}{2l} \right) + 0.5 \right] [46]$$
 (3.2)

Where: L: inductance in  $(\mu H)$ , b: length of the microstrip in (mm), l: width of the microstrip in (mm).

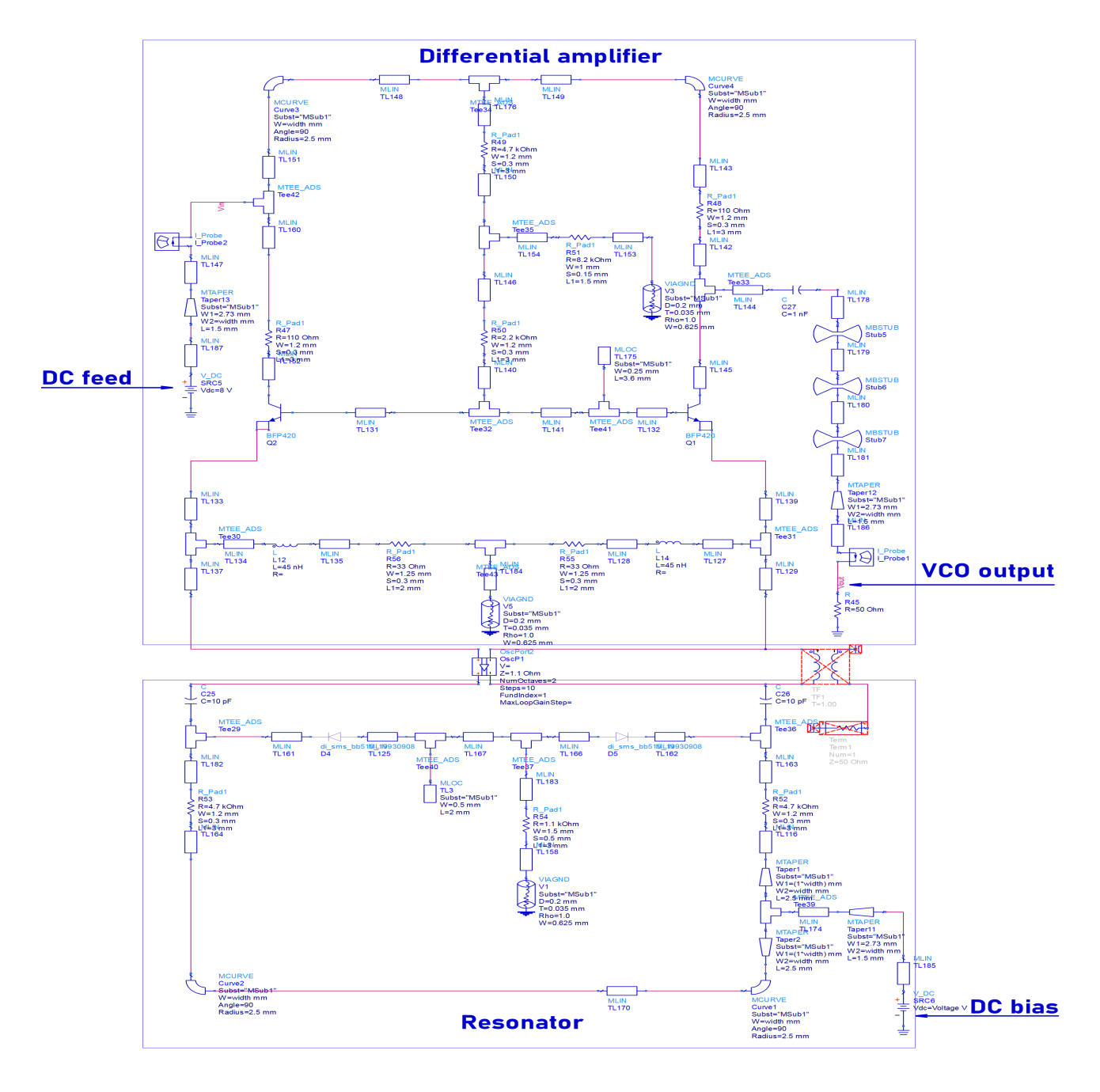


Figure 3.10: The complete circuit of the VCO.

# 3.5 Performance evaluation through simulation

# 3.5.1 Oscillation conditions verification

As seen in figure:3.11, oscillation conditions are verified as the overall imaginary part between the amplifier and the resonator is null, and the real part is always negative over the whole frequency band of the VCO which satisfies the conditions stated in section:2.1.2.

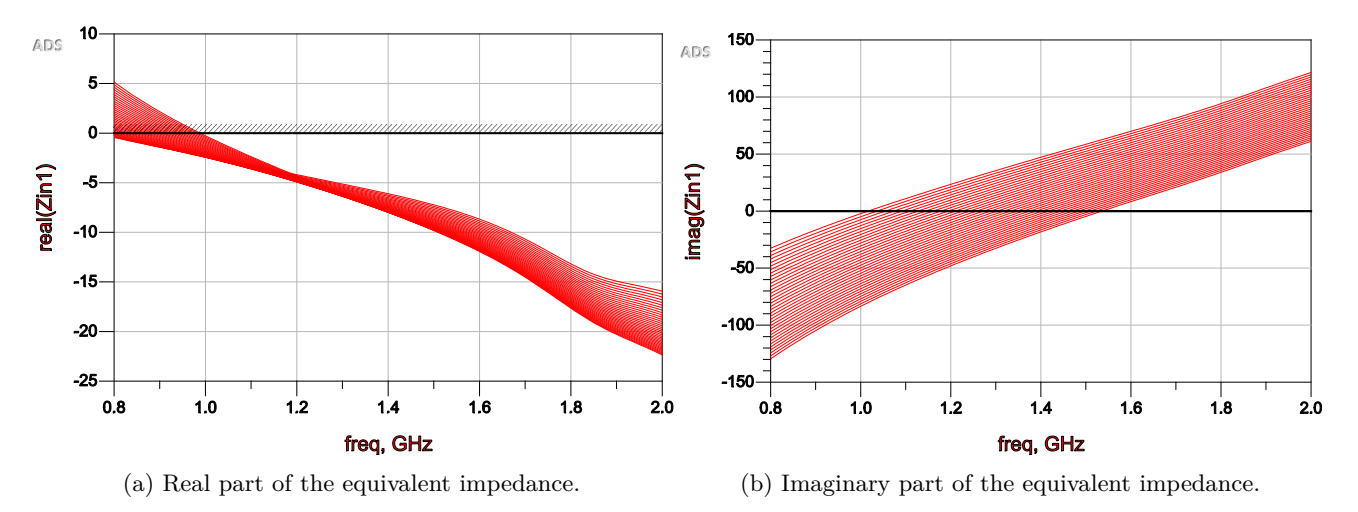


Figure 3.11: Oscillation conditions.

# 3.5.2 Steady-state detection

Steady-state is detected by means of *Oscport*2, that is to detect the predominate deterministic signal flowing through the VCO for each bias voltage value, which promises to have a pure sinusoidal output as shown in figure:3.12.

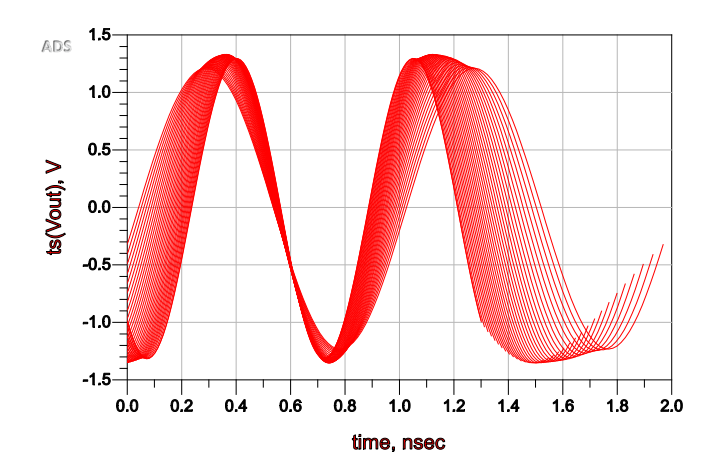


Figure 3.12: Steady state signals detected during simulation.

**Note:** In figure:3.11,3.12, the tuning voltage was varied from 0V to 22V.

## 3.5.3 VCO transfer function

The transfer function of a VCO as explained in section:2.2.2.1 is a parameter that defines the VCOs operating frequency range, observing figure:3.13 it is very clear that the simulated frequency range starts at 1.016GHz achieved at 5V bias voltage, oscillation frequency increases by virtue of the fact that the varactors capacitance decreases as reverse bias voltage increases, at 22V the oscillation frequency is 1.539GHz this is not the real

limit of the band as BB135 diodes can accept up to 30V in reverse bias, the reason of stopping at 22V returns to the fact that the diode model used in ADS software is stopped at 23V, by consequence after that voltage value the simulation diverges and no results are given as well. The real frequency range is going to be discussed in the last chapter.

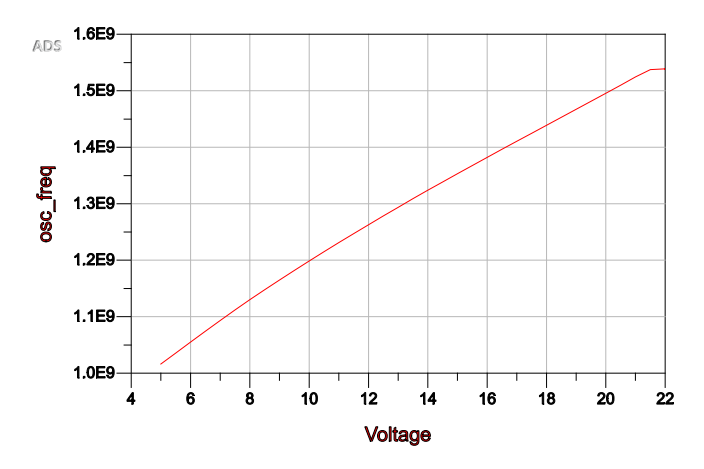


Figure 3.13: Transfer function of the VCO.

Another key parameter could also be extracted from figure:3.13, that is the VCO gain  $K_{VCO}$  also known as tuning sensitivity, that parameter is used to describe the amount of frequency variation with respect to 1V voltage variation, hence it is defined as the approximate slope of the transfer function of the VCO.

$$K_{VCO} = \frac{df_{osc}}{dV_{bias}} = \frac{(1.5 - 1.2)10^9}{20 - 10} \approx 30MHz/volt$$
 (3.3)

# 3.5.4 Output power

The output power is a measure of how strong is the output signal of the VCO, as shown in figure:3.14, the output power of the proposed VCO ranges between 11.75dBm at 5V and 12.56dBm peak at 13.5V, it starts then to decrease as the bias voltage increases, at 22V the VCO exhibits a signal with 12.293dBm

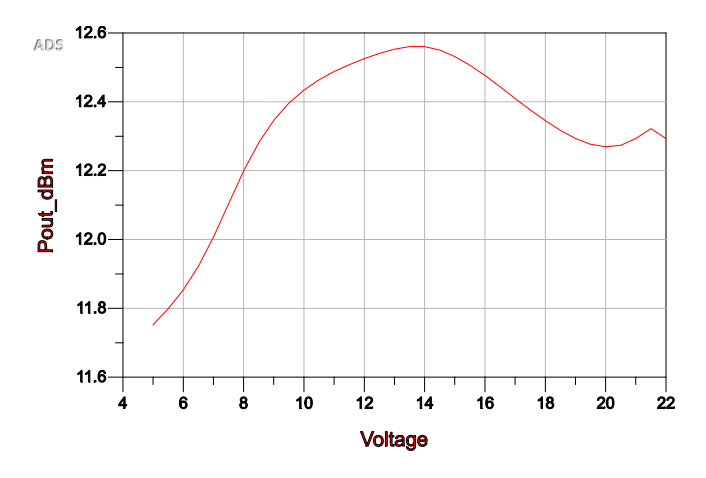


Figure 3.14: Output power of the VCO.

Considering an average output power value, it could be stated that this VCO has as average output power of: 12.321dBm, this is acceptable for a VCO which operates at the L-band.

# 3.5.5 Phase and amplitude noise

Phase noise is the amount of noise power concentrated in 1Hz bandwidth measured at an offset frequency  $\Delta f$  from the carrier, usually the offset is 1MHz, as shown in figure:3.15a at 1MHz offset the phase noise level is below -120dBcHz for all voltage values, that means for all oscillation frequencies, this measure describes the spectral purity around the carrier frequency exhibited by the VCO, if phase noise level is relatively high, it may cause signal distortion, as well as adjacent channel perturbations.

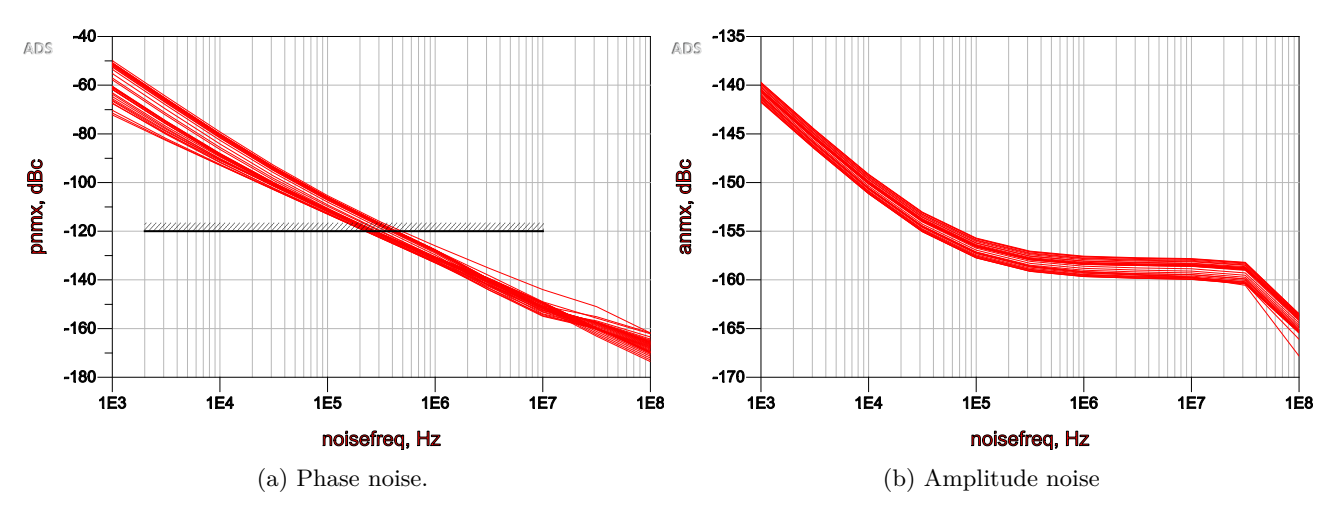


Figure 3.15: VCO noise.

In figure:3.15b it is obvious that amplitude noise is very low as it starts at -140dBcHz, hence it is neglectable in front of phase noise as stated in section:2.2.1.

# 3.5.6 Figure of merit

As VCOs are devices with a variety f key performance parameters, their comparison becomes difficult. A figure of merit is then defined to by pass this comparison problem, according to [47] [48] a highly recommended FOM is mentioned:

$$FOM = \mathcal{L}\{f_{osc}, \Delta f\} - 20log\left[\frac{f_{osc}}{\Delta f}\right] + 10log\left[\frac{P_{supply}}{1mW}\right] [47][48]$$
(3.4)

where:  $f_{osc}$ : oscillation frequency,  $\Delta f$ : offset from the oscillation frequency,  $P_{supplu}$ : Power supply expressed in milliwatts

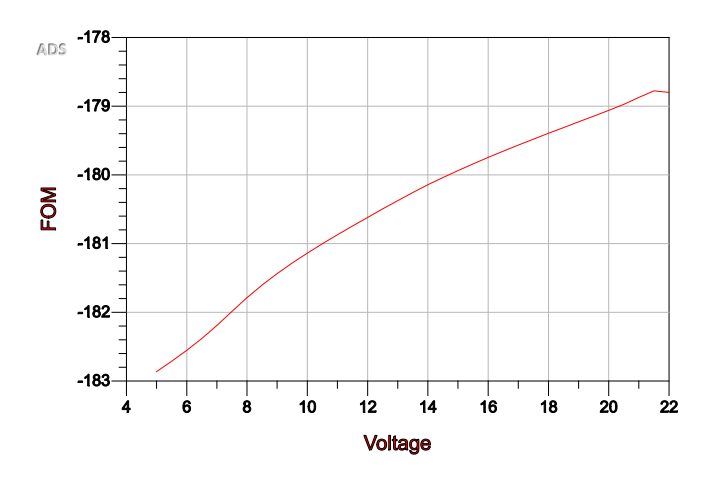


Figure 3.16: Figure of merit of the VCO.

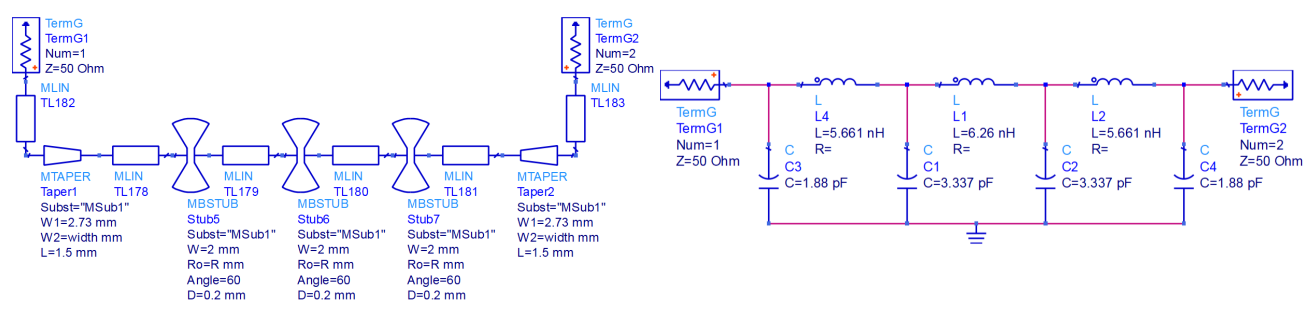
As much as the FOM is low as much as the VCOs performance is high, that is explained by the fact that both quantities  $\mathcal{L}\{f_{osc}, \Delta f\}$  and  $10log\left[\frac{P_{supply}}{1mW}\right]$  are sentenced to be minimized. The FOM illustrated in figure:3.16 is

simulated by means of equation (3.4) in ADS software, as it is seen that the whole curve is under -170dBcHz which is excellent, the phase noise selected was the worst one with -125.978dBc/Hz at 1MHz offset.

# 3.6 Butterfly Low Pass Filter

As a matter of fact the spectrum of the proposed VCO is not pure, which means that spurs and harmonics beyond the upper limit of the frequency tuning range must be filtered, for that reason the filter at the output is used. This device on its own is a third order butterfly LPF, its cut-off frequency is precisely 1.974GHz, the attenuation level at the accepted band is -0.46dB, however in the rejected band it must be lower than -20dB for the reasons mentioned in section:2.2.5 concerning harmonic output power, the butterfly shape is inspired from [49], however the order must be increased to achieve the desired sharp response at 2GHz. The butterfly LPF was designed separately in order to verify its real performance in comparison to simulation, that is to avoid problems generated because of bad filtering at the output.

# 3.6.1 LPF circuits and responses



- (a) Distributed elements filter schematic.
- (b) Lumped components filter schematic.

Figure 3.17: Filter schematics

Figure:3.17b show two LPF's, the left side one is a  $7^{th}$  order distributed butterfly LPF, the one next to it to the right is a  $7^{th}$  order ladder filter used as a theoretical version of the former. The strategy is to simulate both of them and check if the distributed filter response converges to the ladder filter response, this is done as the latter forms the adequate filter used to attenuate high order harmonics and spurs at the VCO output.

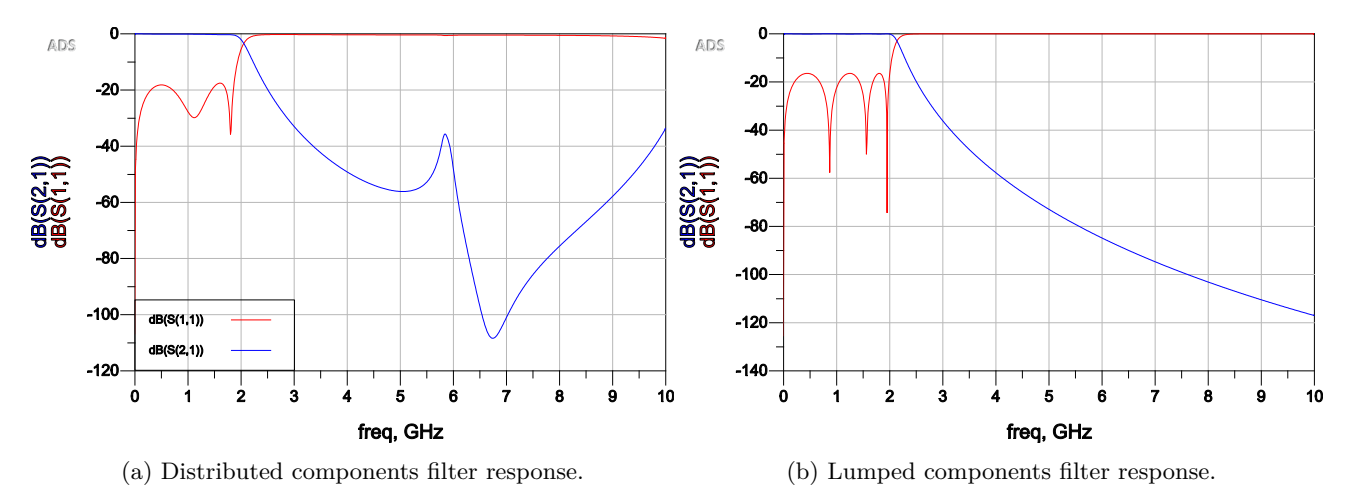


Figure 3.18: Filter responses

As seen in figure:3.18 the butterfly filter response in figure:3.18a converges towards the lumped components filter response shown in figure:3.18b at the frequency band [0-3]GHz, that is enough in our case as higher

order harmonics amplitude decreases exponentially, hence the distributed butterfly filter is suitable to filter the output signal of the proposed VCO.

The butterfly LPF response could be improved further by increasing its order, however the current response fulfills its design purpose. The next step is to generate the layout for that schematic and perform a momentum EM simulation for the sake of comparison with the schematic simulation response illustrated in figure:3.18a.

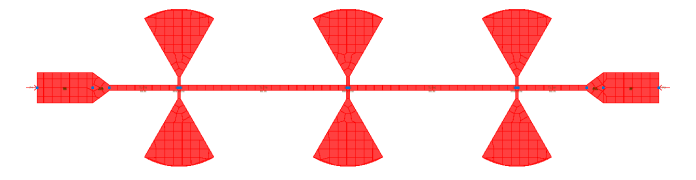


Figure 3.19: Layout design of the butterfly LPF

The EM simulation of the low pass filter structure in figure:3.19 shows similar results to schematic results, improved in terms of sharpness as it achieves the -40dB attenuation level at exactly 3GHz as seen in figure:3.20, this is promising to have a real response similar to simulation as the same response is generated out two distinct simulation mechanisms. After extracting all these results a layout is designed for the VCO as shown in figure: 3.21.

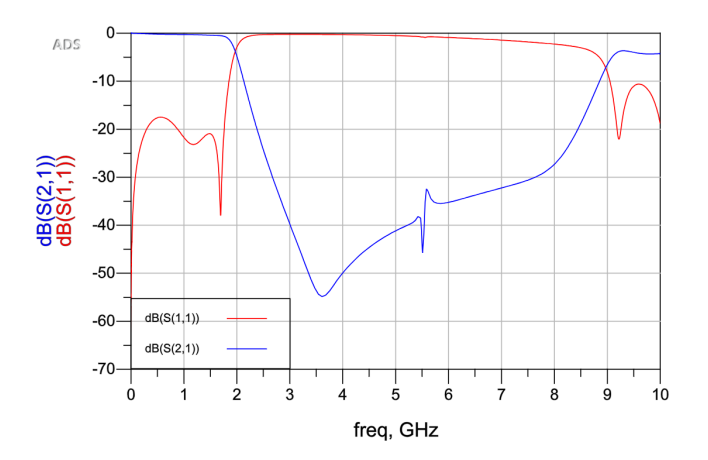


Figure 3.20: Momentum EM response of the butterfly LPF

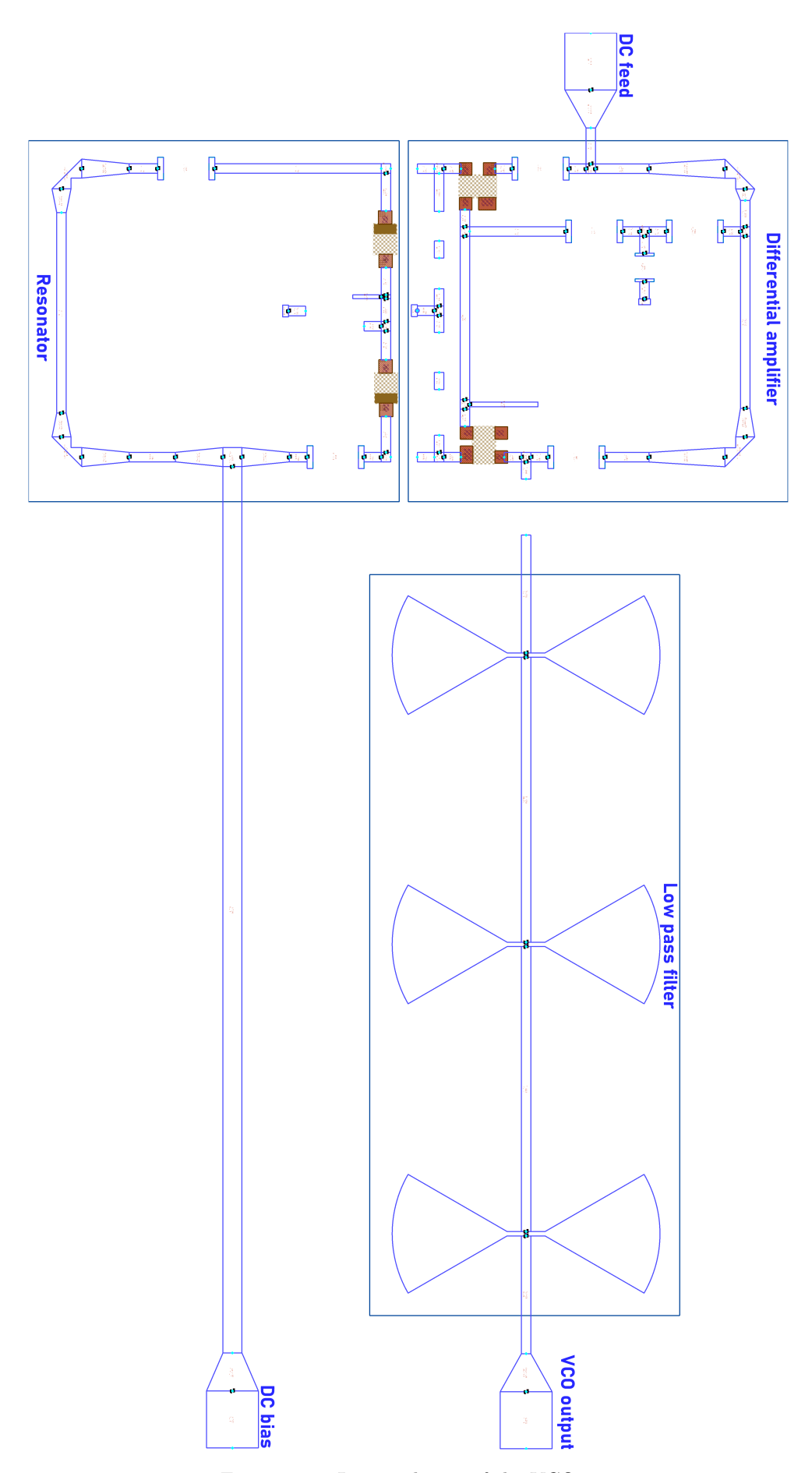


Figure 3.21: Layout design of the VCO.

# Chapter 4

# Implementation, results, and discussion

After the layout design was completed, the implementation process will start, this process begins by printing the layout on a PCB, then soldering components each at its correct position. The detailed process is to be explained in the next sections.

# 4.1 Fabrication process

### 4.1.1 Layout printing and component soldering

Photolithography is a chemical printing technique used to print layouts on PCB's, the method contains several steps, and a mask is necessary to print. In our case the mask is obtained by saving the layout design on a ".dxf" file, this file in then opened using "Autocad" software to adjust the dimensions of the layout, and also to convert the file to ".pdf" extension, the mask is then printed on a transparent film to rise the UV exposure efficiency, as the masks are ready as shown in figure:4.1, the printing process will be initiated.

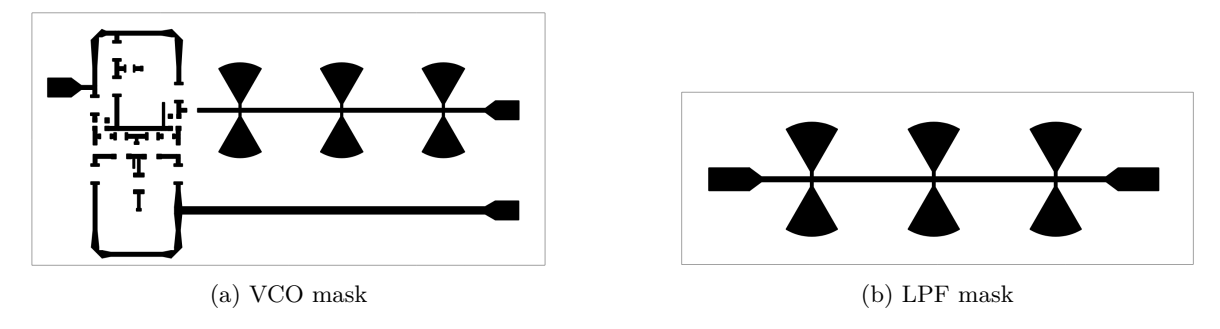


Figure 4.1: Photolithography masks

The layouts are designed on a microstrip board based on FR-4 substrate, covered with copper from each side as seen in figure:4.2, the characteristics of this material are mentioned in table:4.1.

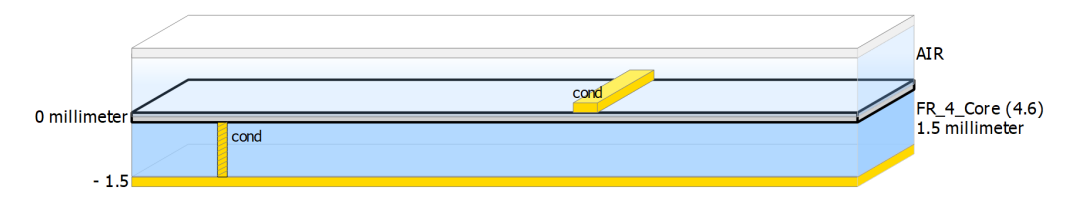


Figure 4.2: Board material

The printing process is done in 5 steps as shown in figure:4.3, the first step is to apply the mask on the board, the latter is then exposed to UV light in order to remove the resist from the top of the copper, the next step is to drown the board inside a basic solution to develop the resist, after that an aside solution is used to

Material parameter	Value
Relative permittivity $\epsilon_r$	4.6
Substrate thickness h	1.5mm
Loss tangent $\delta$	0.019
Trace (conductor) thickness $t$	0.035mm

Table 4.1: Material characteristics

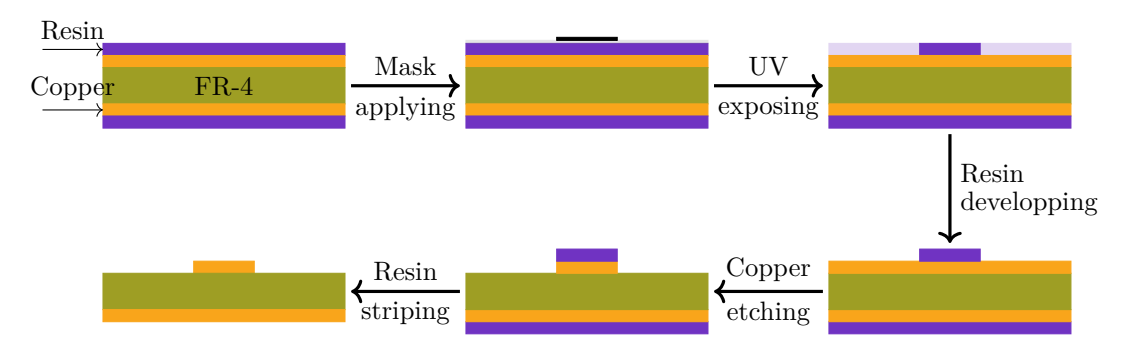


Figure 4.3: Photolithography printing steps

etch copper other than the masked region, the final step is to expose the board again to UV light in order to wash away what is left from the resist on the ground plan and on the masked area.

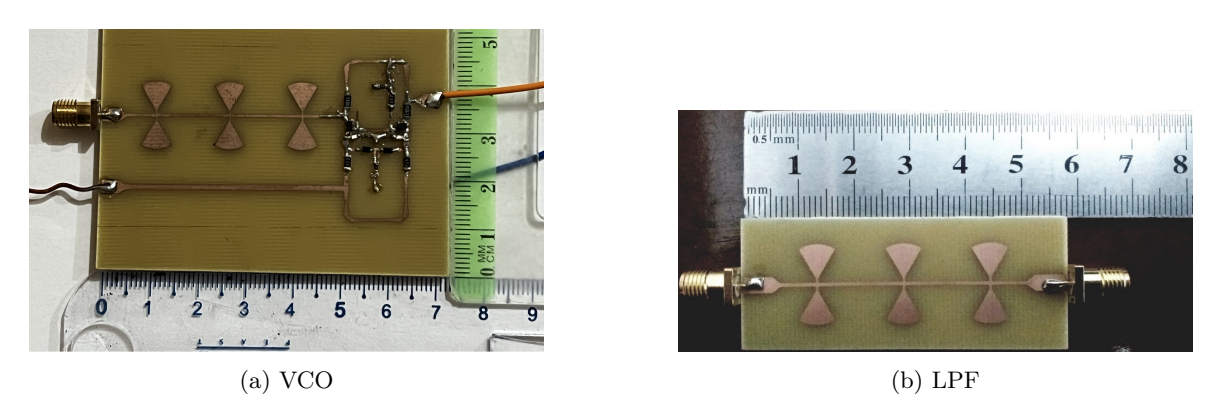


Figure 4.4: Printed circuits

As shown in figure:4.4, both circuits are printed using the photolithography technique, components on the VCO circuit are soldered manually using soldering iron and tin wire, the connectors used are of female SMA type with characteristic impedance  $50\Omega$ , therefore the tapper connections preceding the outputs are used to lower the impedance of transmission line to  $50\Omega$ .

# 4.2 Experimental setups and measurement results

## 4.2.1 LPF measurements

# 4.2.1.1 LPF measurements setup

The butterfly LPF is a two port microwave device, therefore a Vector Network Analyser VNA is needed to perform such measurements, the nano VNA liteVNA 64 is a sufficient device that could provide the frequency response of the LPF as it operates on a range starting from 0.05GHz up to 6GHz, the setup is composed from: the nanoVNA, RF connection cables, and the Device Under Test DUT as shown in the figure:4.5, a calibration process must be done on the VNA to make sure that it is measuring right values at the end its ports,

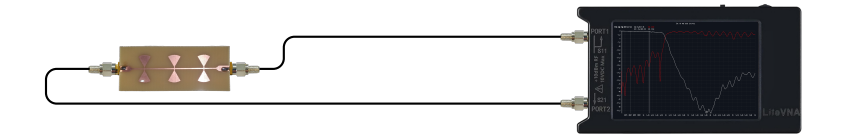


Figure 4.5: LPF measurement setup

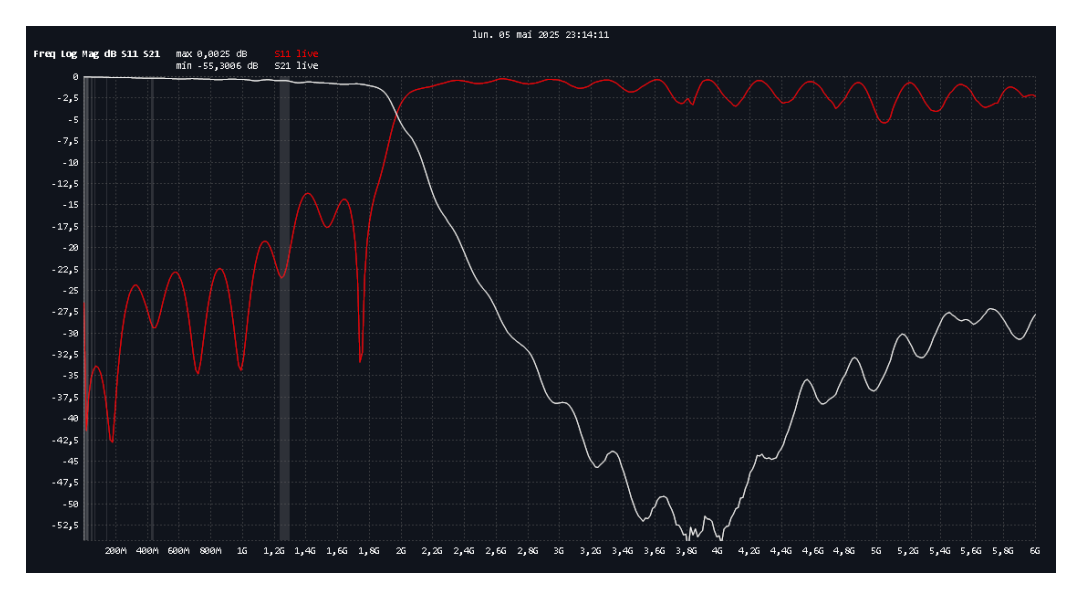


Figure 4.6: NanoVNA LPF measurement results:  $S_{11}$  and  $S_{21}$  parameters

#### 4.2.1.2 LPF measurements results

The calibration process is done in the cable-DUT interface, that is to eliminate the effect of all connectors and cable preceding the LPF. All connectors used in this setup are of type SMA, that eliminates the need for connection adapters. By means of the setup shown in figure:4.5, the results depicted in figure:4.6 are extracted, in comparison to EM simulation results from figure:3.20 a great similarity is observed, the only thing that differs is the level of  $S_{11}$  from 1.35GHz to 1.8GHz as it rises from -20dB to -12.5dB however this is not taken into consideration as an anomaly as its level is under -10dB all across the accepted frequency band, from this comparison the designed filter is capable of fulfilling its purpose in reality.

## 4.2.2 VCO measurements

#### 4.2.2.1 VCO measurement setup

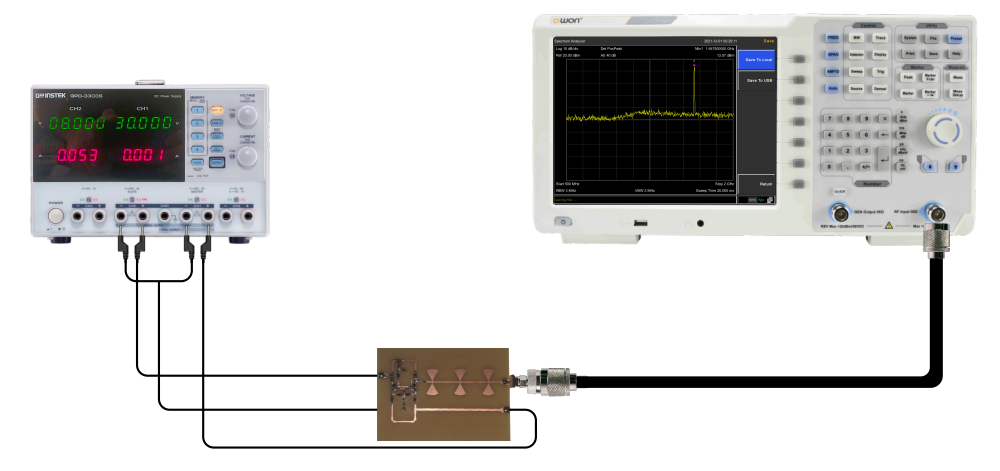


Figure 4.7: VCO measurement setup

As the proposed VCO through this thesis is a linear harmonic VCO, which means that its output signal is always sinusoidal, the primary parameter meant for measurement is the output signal frequency, consequently a setup is prepared to measure this quantity, the latter contains: a spectrum analyser "OWON XSA1036-TG" that the range is [9KHz - 3.6GHz] which makes it an adequate range to measure the output frequency of our VCO, RF connection with N-type connectors from both ends, N-type to SMA adapter to connect the DUT to the spectrum analyser, DC power supply, and lastly the DUT that is the VCO circuit shown in figure:4.4a. The DUT is connected to the spectrum analyser using the N-type to SMA adapter and the RF cable, its DC feed voltage is brought from a DC power supply with two channels, where the second is used for DC tuning voltage.

#### 4.2.2.2 VCO measurement results

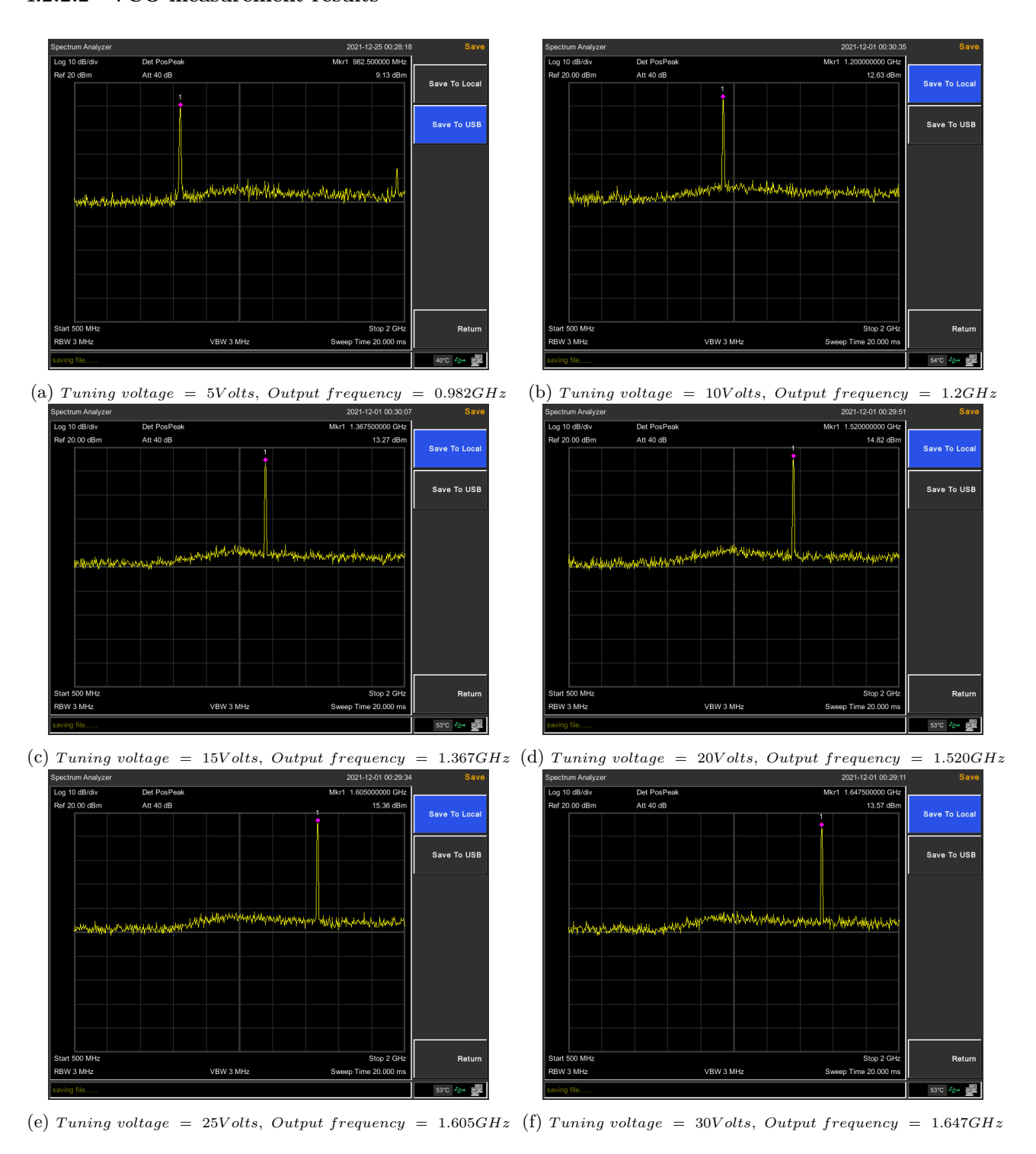


Figure 4.8: Spectrum analyser VCO measurement results: Output frequency and output power

Figure:4.8 shows results from spectrum analyser, it illustrates the tuning voltage variations VS output frequency, the second information that could be extracted from these results is the output power level as the marker "mkr1" indicates both frequency and peak power simultaneously. The second harmonic that appears in figure:4.8a is negligible as its power level with respect to the fundamental is -33.42dBc which is lower than -20dBc [50], consequently its contribution to the output signal is minimal. The contribution of higher order harmonics is also neglected as the harmonic power level in other words harmonics amplitude decays exponentially with frequency increase.

#### 4.2.2.3 Phase noise

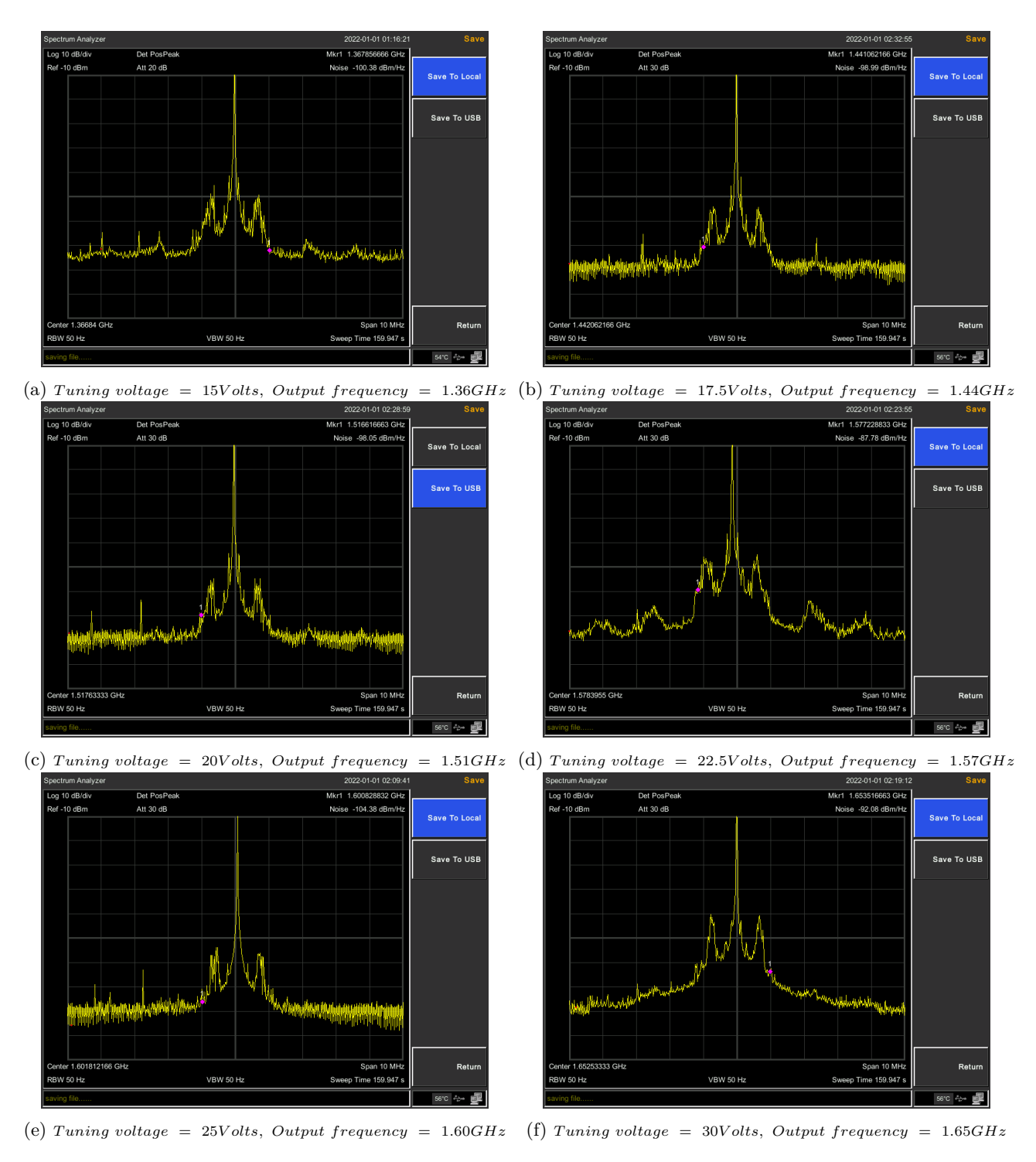


Figure 4.9: Spectrum analyser VCO measurement results: Phase noise

Due to the lack of noise measurement equipment, the spectrum analyser in figure:4.7 is used to measure this key parameter, the strategy is to measure the noise floor at 1MHz offset from the carrier, with 50Hz filter Resolution BandWidth RBW, then to compensate to 1Hz resolution using a correction factor as phase noise is defined as the amount of noise distributed over 1Hz bandwidth. The correction term is  $10log_{10}(K \cdot RBW)$  that is known as the Equivalent Noise BandWidth ENBW, K is the correction factor equals to 1.12 for Gaussian filters, the filter shape is mentioned in the device manual [51], the K factor is obtained from [52] as no information is mentioned about it in [51]. Therefore an elaborated formula to get the correct phase noise level:

$$\mathcal{L}\{1MHz\}[dBm/Hz] = Noise\_power - 10log_{10}(K \cdot RBW)$$
(4.1)

As the latter is measured by a reference to the centre frequency that is in dBc/Hz, the power level of the carrier frequency has to be subtracted:

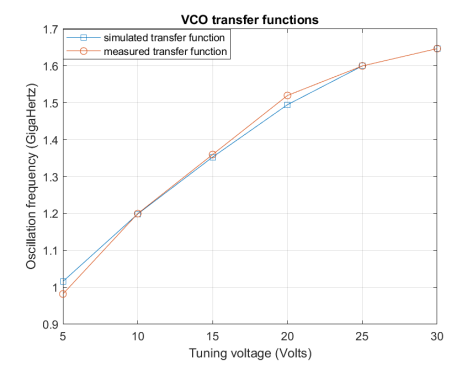
$$\mathcal{L}\{1MHz\}[dBc/Hz] = Noise\_power - 10log_{10}(K \cdot RBW) - Carrier\_power$$
 (4.2)

Frequency $(GHz)$	1.36	1.44	1.51	1.57	1.60	1.65
Carrier power $(dBm)$	13.27	14.1	14.82	15.2	15.36	13.6
Simulated phase noise $(dBc/Hz)$	-129.735	-127.64	-128.527	-126.086	-	-
Measured phase noise $(dBc/Hz)$	-131.13	-130.6	-130.35	-120.46	-137.2	-123.16

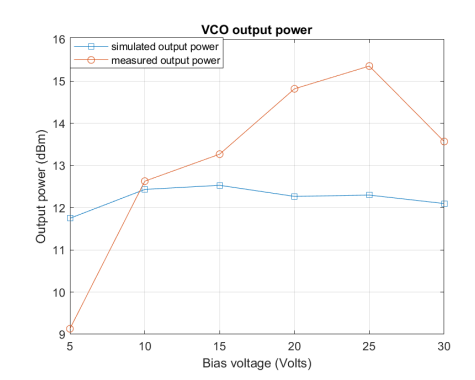
Table 4.2: Simulated and measured phase noise comparison

Table:4.2, is constructed to give an idea about the measured and simulated phase noise levels, as it is seen the measured phased is a little high in comparison to the simulated one, however these values remain acceptable for the proposed VCO as a microstrip strip structure port a lot of noise to the output signal in comparison to to other advanced technologies, the last two values concerning the simulated phase noise are not mentioned because the simulation end at 23V which corresponds to 1.52GHz, this because the diode model in ADS does not possess values beyond 23V. From the values of table:4.2, it is clear that the proposed VCO possess an acceptable phase noise level in comparison to VCOs in [53] [54] [55].

#### 4.2.2.4 Transfer function and output power



(a) Measured and simulated transfer function



(b) Measured and simulated output power

Figure 4.10: Spectrum analyser VCO measurement results: transfer function and output power

Figure:4.10a show a comparison between the measured and simulated transfer functions of the proposed VCO, a high similarity between the curves is shown, which means that measurements match simulation results as desired, consequently it is concluded that the proposed VCO operate at the correct frequency band mentioned in table:3.1. Concerning the measured output power it is not very similar to the simulated one, however that does not make it a poor result as the power levels are convenient for a signal that ranges from 0.9GHz to 1.652GHz [56] [57] [58] [50].

# 4.3 Results validation

According to the previous section of this chapter, measurement results are quit similar to simulation results, concerning: VCO transfer function, output power level, and phase noise. Comparing to real world devices such as: [56] [57] [58] [50] [53] [54] [55], the proposed VCO shows a likewise performance, table:4.3 surmises this comparison clearly, this validates the proposed VCO for its fabrication purposes.

Table 4.3: Comparative table between real world and the proposed device.

VCO device	Part name	Frequency range $[MHz]$	Output power $[dBm]$	Phase noise $[dBc \cdot Hz^{-1} @ 1MHz]$	DC Supply voltage $[V]$	Tuning voltage $[V]$
MAXIM	MAX2754EUA	1145-1250	-5	-124	5.5	0 - 3
ALPHA	APN1006	950-2150	5.7	-	5	0.5 - 30
CRYSTEK	CRBV55BE	1000-2000	9	-141.1714	10	1 - 20
CRYSTEK	CVC055BE	800-1600	7.5	-142.9962	11.5	0.5 - 19
PASTER- NACK	PEV1V31012	1600-3200	6	-130	5	0.5 - 20
PASTER- NACK	PEV1V31020	1070-1210	6	-109 @ 10KHz	12	0.5 - 4.5
PASTER- NACK	PEV1V31026	2400-2800	9	-92 @ 10KHz	12	1 - 11
	This work	982-1650	15.2	-131.13	8	5 - 30

# Conclusion

As a consequence of reading this thesis, a one had the overall experience of developing an L-band VCO, where they encountered all kinds of VCO technologies. In the first chapter including microstrip, stripline, waveguide, and CMOS VCO's. The second chapter took as a topic the explanation of the principle of operation of oscillators which were the linear feedback and negative resistance approaches. In addition to that, the chapter introduced the key performance parameters of a voltage controlled oscillator. The third chapter positioned the proposed VCO circuit where we introduced the readers to its design process then simulation using ADS software and finally simulation results, were the difficulty to guarantee oscillation conditions was faced. The last chapter was completely consecrated for the implementation, measurement results and comparisons, hence all steps of microwave VCO design using microstrip technology were mentioned in this thesis. The components used to fabricate the VCO circuit were recovered from an old motherboard by means of a heating process theses includes resistors only in the exception of the  $27\Omega$  once, all other components including inductors, capacitors, transistors, and varactor diodes, these were obtained from china. The proposed VCO had a tuning range starting from 0.982GHz ending at 1.647GHz, consequently its tuning bandwidth is 665MHz, its output power is relatively high with an average of 13.13dBm, another crucial parameter that has to be taken care of specially in radar systems is the phase noise, the proposed VCO exhibits signals with an average phase noise level of  $-128.81dBc \cdot Hz^{-1}$  which is acceptable, however its spectrum suffers from the sideband spurs seen in figure: 4.9, these spurs are not to worried about as their power level is very relatively to the centre frequency power level.

Upon considering all the facts, the problematic of this humble thesis was to design, simulate, and implement a voltage controlled oscillator for L-band applications, the results depicted in chapter number four describes the success of the proposed VCO circuit in solving the posed problematic, hence and by means of measurement results as they were identical to simulation results up to some point of similarity, the simulation phase is validated, consequently the proposed VCO circuit fulfils its implementation purpose correctly.

Speaking of the future, the prospects of this thesis is to improve its design especially the output filter size as it occupies half the size of the complete VCO board, much further a one may think of designing integrated microwave VCOs using CMOS technology as they are known for their compactness, low supply power, and high frequencies.

# Bibliography

- [1] Lockheed Martin Rotary and Mission Systems. TPS-77 MRR Multi-Role Radar.
- [2] Lockheed Martin Rotary and Mission Systems. TPY-4 Multi-Mission Radar.
- [3] Kratos Defense & Security Solutions Inc. L-band ATC Antenna.
- [4] Ahmed Salama, Osama Dardeer, Angie Eldamak, and Hadia El-Henawy. Compact dual-band cpw-fed circularly polarized slot antenna for gnss applications. Progress In Electromagnetics Research C, 149:187–197, 01 2024.
- [5] Anonymous Author. Ieee standard letter designations for radar-frequency bands ieee aerospace and electronic systems society developed by the radar systems panel | institute of electrical and electronics engineers, 11 2019.
- [6] Bryant Derand Williamson. A 2.4 ghz lc-vco using on-chip inductors and accumulation-mode varactors in a cmos 0.18 um process. Master's thesis, University of Tennessee, 2005.
- [7] N4GG Hal Kennedy. How spark transmitters work.
- [8] E.H. Armstrong. The super-heterodyne-its origin, development, and some recent improvements. *Proceedings* of the Institute of Radio Engineers, 12(5):539–552, 1924.
- [9] Alfred.T Witts. Super heterodyne receiver. Issac Pitman, 1961.
- [10] BARNES SANFORD H; MANN JOHN E. Voltage sensitive semiconductor capacitor. https://world-wide.espacenet.com/patent/search/family/024963580/publication/US2989671A?q=pn
- [11] Ioannis Sarkas, Juergen Hasch, Andreea Balteanu, and Sorin P. Voinigescu. A fundamental frequency 120-ghz sige bicmos distance sensor with integrated antenna. *IEEE Transactions on Microwave Theory and Techniques*, 60(3):795–812, 2012.
- [12] Electronic warfare. https://www.lockheedmartin.com/en-us/capabilities/electronic-warfare.html.
- [13] What is a function generator? https://www.keysight.com/used/us/en/knowledge/ glossary/oscilloscopes/what-is-a-function-generator.
- [14] Behzad Razavi. Design of Analog CMOS Integrated Circuits. McGraw-Hill Education Europe, 2015.
- [15] Hanqiao Zhang, Steven Krooswyk, and Jeffrey Ou. High Speed Digital Design: Design of high speed interconnects and signaling. Morgan Kaufmann is an imprint of Elsevier, 2015.
- [16] 200-05911-0010 stripline vco board assembly (new old stock) (sa). https://baspartsales.com/200-05911-0010-stripline-vco-board-assembly-new-old-stock-sa/.
- [17] Matjaz Vidmar. Wide-band & low-noise microwave vco. https://lea.hamra-dio.si/s53mv/spectana/vco.html.

- [18] What is a complementary metal oxide semiconductor (cmos)? https://www.keysight.com/used/us/en/knowledge/glossary/oscilloscopes/what-is-a-complementary-metal-oxide-semiconductor-cmos.
- [19] CHEN ZHAO WENQI CAI XIAO MO JUN YUAN GUANYU WANG WEI WANG, YAO LIANG. Quiet vco tunes 2.5-ghz wimax. Master's thesis, College of Electronics Engineering, Chongqing University of Posts and Telecommunications, 2014.
- [20] David M. Pozar. Microwave Engineering Fourth Edition. John Wiley & Sons, 2012.
- [21] T. Baek, Dongsik ko, Sujin Lee, Yong-Hyun Baek, Min Han, Seok Choi, Jae-Hyun Choi, Wan-Joo Kim, and Jin-Koo Rhee. A transceiver module for fmcw radar sensors using 94-ghz dot-type schottky diode mixer. Sensors Journal, IEEE, 11:370 376, 03 2011.
- [22] N. R. Sivaraaj and K. K. Abdul Majeed. A comparative study of ring vco and lc-vco: Design, performance analysis, and future trends. *IEEE Access*, 11:127987–128017, 2023.
- [23] SORIN VOINIGESCU. High-Frequency Integrated Circuits. cambridge university press, 2013.
- [24] Chen Huifang, Wang Xiantai, Xiaojuan Chen, Luo Weijun, and Liu Xinyu. An 8 ghz high power algan/gan hemt vco. *Journal of Semiconductors*, 31:074012, 07 2010.
- [25] Izzat Darwazeh Clive Poole. *Microwave Active Circuit Analysis and Design*. Academic press, Elsevier, 2016.
- [26] D.B. Leeson. A simple model of feedback oscillator noise spectrum. *Proceedings of the IEEE*, 54(2):329–330, 1966.
- [27] Enrico Rubiola and Vincent Giordano. On the 1/f frequency noise in ultra-stable quartz oscillators. *IEEE Transactions on Ultrasonics, Ferroelectrics, and Frequency Control*, 54(1):15–22, 2007.
- [28] Stephen A. Maas. Nonlinear microwave and RF circuits. Artech House, 2003.
- [29] David P. Newkirk Ulrich L. Rohde. *RF/MICROWAVE CIRCUIT DESIGN FOR WIRELESS APPLICA-TIONS*. JOHN WILEY & SONS, 2000.
- [30] S.IIAMIDNAWAB ALAN v. OPPENHEIM, ALAN s. wILLSKY. Signals & systems. PRENTICE-HALL INTERNATIONAL, INC, 1996.
- [31] Jae-Sung Rieh. Introduction to Terahertz Electronics. Springer, 2021.
- [32] Ravish Aradhya H V. BASIC ELECTRONICS. McGraw Hill Education, 2013.
- [33] Dielectric resonator oscillator (dro). https://www.microwave-jh.com/dro.html.
- [34] Randall W.Rhea. Discrete Oscillator Design: Linear, Nonlinear, Transient, and Noise Domains. Logo Publisher, 2010.
- [35] Darko Kajfezand Pierre Guillon. Dielectric resonators. NOBLE publishing corporation, 1998.
- [36] Eric Vittoz. Low-Power Crystal and MEMS Oscillators The Experience of Watch Developments. Springer, 2010.
- [37] A comprehensive guide to mems oscillators. https://nz.rs-online.com/web/content/discovery/ ideas-and-advice/mems-oscillators-guide?srsltid=AfmBOorbmCGxexKXHrCQWpQCF9Legsj4OVMarhAKJMIefxZ vJJoGIN-C.
- [38] Ramon M. Cerda. Understanding Quartz Crystals and Oscillators. ARTECH HOUSE, 2014.

- [39] Empro 2015.01 product release. https://www.keysight.com/us/en/lib/resources/software-releases/empro-201501.html.
- [40] Empro 2017 product release. https://www.keysight.com/us/en/lib/resources/software-releases/empro-2017.html.
- [41] N Suresh Kumar S Salivahanan. ELECTRONIC CIRCUITS 1. McGraw Hill Education (India), 2018.
- [42] Infineon Technologies AG. Surface mount wideband silicon NPN RF bipolar transistor, 01 2019. Revision 3.0.
- [43] Peter C.L. Yip. High-Frequency Circuit Design and Measurements. CHAPMAN & HALL, 1990.
- [44] PHILIPS. UHF variable capacitance diode, 09 1998.
- [45] Keysight, 5301 Stevens Creek Blvd., Santa Clara, CA 95052 USA. Measurement Expressions, 2011.
- [46] Pcb inductors. https://coil32.net/pcb-coil.html.
- [47] Y.-C Lin, Mei Yeh, and C.-C Chang. A high figure-of-merit low phase noise 15-ghz cmos vco. *Journal of Marine Science and Technology (Taiwan)*, 21:82–86, 02 2013.
- [48] Marc Tiebout. Low power VCO design in CMOS. Springer, 2006.
- [49] Sohrab Majidifar and Mohsen Hayati. Design of a sharp response microstrip lowpass filter using taper loaded and radial stub resonators. TURKISH JOURNAL OF ELECTRICAL ENGINEERING & COMPUTER SCIENCES, 25:4013–4022, 01 2017.
- [50] MAXIM. 1.2GHz VCO with Linear Modulation Input, 2006. Revision 2.
- [51] OWON. XSA1000 Series Spectrum Analyzer User Manual, 09 2020.
- [52] How does the noise marker function work on my spectrum analyzer? https://docs.keysight.com/kkbopen/how-does-the-noise-marker-function-work-on-my-spectrum-analyzer-577940563.html.
- [53] PASTERNACK. Voltage Controlled Oscillator (VCO) From 1.6 GHz to 3.2 GHz, Phase Noise of -89 dBc/Hz and SMA, 2017. Revision: 1.1.
- [54] PASTERNACK. Voltage Controlled Oscillator, 1070 MHz to 1210 MHz, Pout +1.5 dBm, Phase Noise of -109 dBc/Hz, 0.5V to 4.5V Tuning Range, SMA, 2020. Revision: 1.0.
- [55] PASTERNACK. Voltage Controlled Oscillator, 2400 MHz to 2800 MHz, Pout +9 dBm, Phase Noise of -92 dBc/Hz, 1V to 11V Tuning Range, SMA, 2020. Revision: 1.0.
- [56] Alpha Industries. A Colpitts VCO for Wideband (0.95-2.15 GHz) Set-Top TV Tuner Applications, 1999.
- [57] CRYSTEK MICROWAVE. Voltage Controlled Oscillator-VCO CVCO55CW-1000-2000, 12 2016. Revision:K.
- [58] CRYSTEK MICROWAVE. Voltage Controlled Oscillator-VCO CVCO55BE-0800-1600, 08 2020. Revision: H.